Converted PS-wave reflection coefficients in anisotropic media

Petr Jílek
Center for Wave Phenomena, Colorado School of Mines

ABSTRACT

I derive converted PS-wave reflection coefficients at a horizontal weak-contrast interface separating two weakly anisotropic halfspaces using first-order perturbation theory. The general expressions are further specified for the interface between any of the two following media: isotropic, VTI, HTI or orthorhombic. Relatively simple forms of small-angle reflection coefficients are also obtained. The results are expressed as functions of Thomsen-type medium parameters and incidence and azimuthal angles.

Derived expressions, as well as their application, are more complicated than the corresponding expressions for PP-wave reflection coefficients. Some general characteristics and pitfalls are discussed. Numerical tests reveal a good agreement between exact and approximate coefficients for most tested models.

Introduction

Amplitude-variation-with-offset (AVO) analysis is frequently used in seismic exploration as a method for direct detection of hydrocarbons. Continual development of AVO techniques helps to improve estimates of such properties of hydrocarbon reservoirs as porosity, crack density, orientation of cracks, fluid content etc.

The crucial quantity in AVO analysis is the reflection coefficient at the target horizon, such as the top of a hydrocarbon reservoir, as a function of incidence angle and azimuth. Analytic expressions for reflection and transmission coefficients of plane waves for a planar interface separating two isotropic halfspaces have been derived in the past by several authors, for example Zoeppritz (1919), Červený *et al.* (1977) and Aki & Richards (1980). In the presence of anisotropy, reflection and transmission coefficients generally become complicated functions of elastic parameters and the direction of wave propagation, and, except for some higher anisotropic symmetries, must be treated numerically (Musgrave, 1970; see also Daley and Hron, 1977, Keith & Crampin, 1977, or Graebner, 1992).

Due to the complexity of exact reflection and transmission coefficients, their approximations are of great importance in practical AVO analysis. The approximations are commonly based on the assumption of a weak contrast of the elastic medium parameters across the interface, which allows one to linearize the exact expressions in those parameters. Some approximate analytic expressions for reflection and transmission coefficients for isotropic models can be found in Bortfeld (1961), Richards & Frasier (1976), Aki & Richards (1980) and Shuey (1985).

For anisotropic models, a derivation of such approximations is significantly more complicated, and usually includes the additional assumption of a weak anisotropy in both halfspaces (above and below the interface). P-wave reflection coefficient for weakly anisotropic VTI media and small incidence angles was first introduced by Banik (1987) and later extended for larger incidence angles by Thomsen (1993). Rüger (1996, 1997 and 1998) refined Thomsen's (1993) expression and derived the complete set of approximate reflection and transmission coefficients for VTI media and for symmetry planes of HTI and orthorhombic media (with aligned vertical symmetry planes in the incidence and reflecting halfspaces). Also, he derived azimuthally dependent P-wave reflection coefficient for an interface between two HTI media. Pšenčík and Vavryčuk (1998) and Vavryčuk and Pšenčík (1998) presented azimuthally dependent weak-contrast, weak-anisotropy P-wave reflection/transmission coefficients for arbitrarily anisotropic halfspaces. Vavryčuk (1999) also shows general forms of converted PS-wave reflection coefficient approximations. Those forms, how-

ever, are not well suited for AVO analysis in typical anisotropic media.

The work discussed above is almost entirely devoted to pure P-wave mode reflections. However, recent development of acquisition techniques, such as ocean bottom cable (OBC) surveys, makes it possible to collect high-quality 3-D 3-C data, and thus a joint P- and S-wave analysis becomes realistic. In terms of AVO, analysis of converted PS-wave reflection coefficients may provide important additional information (Jin, 1999; Miley, 1999) without almost any additional cost. For isotropic media, approximate forms of PS-wave reflection coefficients are described in Donati (1998), Larsen *et al.* (1999), Alvarez *et al.* (1999) and Nefedkina and Buzlukov (1999). Li *et al.* (1996) tried to explain the influence of gas saturation and fracturing on PP- and PS-wave reflection coefficients using approximations derived for symmetry-plane reflection at an HTI/HTI interface. To my knowledge, however, general closed-form approximations of R_{PS} coefficients for anisotropic models have not been published.

In this paper, I derive azimuthally dependent weak-contrast, weak-anisotropy PS-wave reflection coefficients for a horizontal interface separating two arbitrarily anisotropic halfspaces. The resulting formulas are further specified for any combination of the following halfspaces: isotropic, VTI, HTI and orthorhombic. An arbitrary azimuth of vertical symmetry planes is allowed in the case of HTI and orthorhombic media. The coefficients are written as functions of Thomsen-type medium parameters (Thomsen, 1986, and Tsvankin, 1997a, 1997b), and incidence and azimuthal angles. Accuracy of the approximations is tested on several numerical examples.

Analytic development

In this section, I derive a linearized form of the plane PS-wave reflection coefficients for arbitrarily anisotropic media. I follow the approach of Vavryčuk and Pšenčík (1998) introduced for PP-wave reflection coefficients, which is based on the assumption of a weak contrast of the elastic parameters across the planar interface, and weak anisotropy of both halfspaces. These assumptions allow one to use first-order perturbation theory (Jech and and Pšenčík, 1989) and linearize exact expressions for both PP- and PS-wave reflection coefficients.

Exact solution of the reflection/transition problem

Let us consider a planar interface with the normal $\boldsymbol{n}$ separating two homogeneous arbitrarily anisotropic halfspaces with densities $\rho^{(1)}$, $\rho^{(2)}$ and the density-normalized stiffness tensor elements $a^{(1)}_{ijkl}$ and $a^{(2)}_{ijkl}$. A harmonic plane wave incident from the halfspace denoted as 1 generates three reflected and three transmitted waves P, S_1 and S_2. The displacement vector of each wave can be written as

$$\boldsymbol{u}^{(N)}(\boldsymbol{x},t) = U^{(N)}\boldsymbol{g}^{(N)}\exp[-i\omega(t-\boldsymbol{p}^{(N)}\cdot\boldsymbol{x})], \tag{1}$$

where $N=0$ corresponds to the incidence wave, $N=1,2,3$ correspond to the reflected S_1, S_2 and P waves and $N=4,5,6$ correspond to the transmitted S_1, S_2 and P waves, respectively. $U^{(N)}$ denotes the scalar amplitude (generally a complex number), $\boldsymbol{g}^{(N)}$ represents the unit polarization vector of the wave N, $\boldsymbol{p}^{(N)}$ is the corresponding slowness vector and ω is the circular frequency. The traction vectors associated with the displacement vectors (1) are

$$\boldsymbol{T}^{(N)}(\boldsymbol{x},t) = i\omega\, U^{(N)}\boldsymbol{X}^{(N)}, \tag{2}$$

where $\boldsymbol{X}^{(N)}$ is so called *amplitude normalized* traction vector,

$$\begin{aligned} X_i^{(N)} &= \rho^{(1)}a^{(1)}_{ijkl}n_j g_k^{(N)}p_l^{(N)}, \qquad N=0,1,2,3, \\ X_i^{(N)} &= \rho^{(2)}a^{(2)}_{ijkl}n_j g_k^{(N)}p_l^{(N)}, \qquad N=4,5,6. \end{aligned} \tag{3}$$

In equation (3), Einstein summation convention applies.

For welded contact between the halfspaces, displacement and traction fields must be continuous across the interface. These two sets of boundary conditions constrain the amplitudes of reflection/transmission waves for a given incident wave. The boundary conditions can be written in a compact matrix form as follows:

$$\hat{\mathbf{C}}\cdot\boldsymbol{U} = \boldsymbol{B}. \tag{4}$$

The right-hand side vector

$$\boldsymbol{B} = -(g_1^{(0)}, g_2^{(0)}, g_3^{(0)}, X_1^{(0)}, X_2^{(0)}, X_3^{(0)})^T \tag{5}$$

corresponds to the incidence wave of the amplitude $U^{(0)}=1$ (the superscript T denotes the transpose). Also, the 6x6 matrix

$$\hat{\mathbf{C}} = \begin{bmatrix} g_1^{(1)} & g_1^{(2)} & g_1^{(3)} & -g_1^{(4)} & -g_1^{(5)} & -g_1^{(6)} \\ g_2^{(1)} & g_2^{(2)} & g_2^{(3)} & -g_2^{(4)} & -g_2^{(5)} & -g_2^{(6)} \\ g_3^{(1)} & g_3^{(2)} & g_3^{(3)} & -g_3^{(4)} & -g_3^{(5)} & -g_3^{(6)} \\ X_1^{(1)} & X_1^{(2)} & X_1^{(3)} & -X_1^{(4)} & -X_1^{(5)} & -X_1^{(6)} \\ X_2^{(1)} & X_2^{(2)} & X_2^{(3)} & -X_2^{(4)} & -X_2^{(5)} & -X_2^{(6)} \\ X_3^{(1)} & X_3^{(2)} & X_3^{(3)} & -X_3^{(4)} & -X_3^{(5)} & -X_3^{(6)} \end{bmatrix} \tag{6}$$

contains quantities constrained by the incidence wave. However, the polarization vectors $\boldsymbol{g}^{(N)}$ and slowness vectors $\boldsymbol{p}^{(N)}$, which are needed for evaluation of the amplitude-normalized traction vectors $X_i^{(N)}$ [equation (3)] in the matrix $\hat{\mathbf{C}}$, must be determined by solving the Christoffel equation,

$$(a_{ijkl}p_i^{(N)}p_l^{(N)} - \delta_{jk})g_j^{(N)} = 0. \tag{7}$$

In general, the system (7) has to be solved numerically. Finally, the vector

$$\boldsymbol{U} = (R_{S1}, R_{S2}, R_P, T_{S1}, T_{S2}, T_P)^T \tag{8}$$

contains the reflection/transmission coefficients to be found. This vector has to be determined by solving the matrix equation (4), together with the Christoffel equation (7). Clearly, for arbitrarily anisotropic media it is impossible to obtain an exact closed-form solution for reflection/transmission coefficients.

First-order perturbation of the exact solution

In this section, I apply first-order perturbation theory to equation (4) which leads to an approximate analytic solution for the reflection/transmission vector $\boldsymbol{U}$. This approach, introduced for generally anisotropic media by Vavryčuk and Pšenčík (1998), is in principle identical to that used by Thomsen (1993) or Rüger (1996). The key difference from Thomsen's or Rüger's approach is a different parameterization of the medium.

As an auxiliary step, let us consider a homogeneous isotropic full space separated by a fictitious planar interface into two halfspaces characterized by the same density ρ^0 and an identical set of density-normalized stiffness coefficients

$$a^0_{ijkl} = (\alpha^2 - 2\beta^2)\delta_{ij}\delta_{kl} + \beta^2(\delta_{ik}\delta_{jl} + \delta_{il}\delta_{jk}), \tag{9}$$

where α and β represent the P- and S-wave velocities. Here, such an isotropic medium is called the *background* medium. The elastic medium parameters of the true halfspaces under consideration can then be expressed in terms of perturbations from the background medium as

$$\begin{aligned} a^{(I)}_{ijkl} &= a^0_{ijkl} + \delta a^{(I)}_{ijkl}, \\ \rho^{(I)} &= \rho^0 + \delta\rho^{(I)}, \end{aligned} \tag{10}$$

where I=1,2 denote the incidence and reflecting halfspaces, respectively. Further, let us assume that the perturbations $\delta a^{(I)}_{ijkl}$ and $\delta\rho^{(I)}$ for both I=1,2 are small, i.e.

$$|\delta a^{(I)}_{ijkl}| \ll ||a^0_{ijkl}||, \qquad |\delta\rho^{(I)}| \ll \rho^0, \tag{11}$$

where the norm $||a^0_{ijkl}||$ can be defined, for example, as $||a^0_{ijkl}|| = \max|a^0_{ijkl}|$. Conditions (11) result in a significant simplification of the exact problem (4), leading to an approximate analytic solution.

Clearly, in order to satisfy conditions (11), the contrasts of the elastic parameters a_{ijkl} and densities ρ across the interface must be small. However, the weak-contrast assumption itself is not the only condition required to satisfy relations (11) for the parameters a_{ijkl}. It must be supplemented by the assumption of weak anisotropy in both halfspaces; otherwise, the perturbations from the isotropic background could be large.

Under the adopted weak-contrast, weak-anisotropy assumption, the polarization and slowness vectors $\boldsymbol{g}^{(N)}$, $\boldsymbol{p}^{(N)}$ from equation (1) can be written in a linearized form as

$$\begin{aligned} \boldsymbol{g}^{(N)} &\approx \boldsymbol{g}^{0(N)} + \delta\boldsymbol{g}^{(N)}, \\ \boldsymbol{p}^{(N)} &\approx \boldsymbol{p}^{0(N)} + \delta\boldsymbol{p}^{(N)}, \end{aligned} \tag{12}$$

where $\boldsymbol{g}^{0(N)}$ and $\boldsymbol{p}^{0(N)}$ are the polarization and slowness vectors of the plane wave of the type N propagating in the background medium, and $\delta\boldsymbol{g}^{(N)}$ and $\delta\boldsymbol{p}^{(N)}$ are their linear perturbations. Using the results of Jech and Pšenčík (1989), Vavryčuk and Pšenčík (1998) derived analytic expressions for the perturbations $\delta\boldsymbol{g}^{(N)}$ and $\delta\boldsymbol{p}^{(N)}$ as linear functions of the perturbations $\delta a^{(I)}_{ijkl}$ introduced in equations (10) and (11). Notice that the non-zero perturbations in equations (12) are due to both the parameter contrasts across the interface and the anisotropy in both halfspaces.

Perturbation equations (10) and (12) also help to linearize the normalized traction vectors $\boldsymbol{X}^{(N)}$ given by equations (3) and, consequently, the matrix $\hat{\mathbf{C}}$ and vectors $\boldsymbol{B}$ and $\boldsymbol{U}$ defined by relations (6), (5) and (8):

$$\begin{aligned} \boldsymbol{X}^{(N)} &= \boldsymbol{X}^{0(N)} + \delta\boldsymbol{X}^{(N)}, \\ \hat{\mathbf{C}} &= \hat{\mathbf{C}}^0 + \delta\hat{\mathbf{C}}, \\ \boldsymbol{B} &= \boldsymbol{B}^0 + \delta\boldsymbol{B}, \\ \boldsymbol{U} &= \boldsymbol{U}^0 + \delta\boldsymbol{U}. \end{aligned} \tag{13}$$

Substituting equations (13) into (4) and keeping only linear terms, we arrive at the final matrix equation for the perturbed vector of the reflection/transmission coefficients:

$$\delta\boldsymbol{U} = (\hat{\mathbf{C}}^0)^{-1}(\delta\boldsymbol{B} - \delta\hat{\mathbf{C}}\cdot\boldsymbol{U}^0). \tag{14}$$

The background vector $\boldsymbol{B}^0$ in equation (14) vanishes due to the fact that $\hat{\mathbf{C}}^0\cdot\boldsymbol{U}^0 = \boldsymbol{B}^0$. In principle identical equation (14) has been derived by Banik (1987) and Thomsen (1993) for VTI media.

Since the background medium is a uniform full space, a fictitious interface in such a medium generates only one transmitted wave of the same type as the incidence wave. Thus, the perturbed reflection/transmission vector $\delta\boldsymbol{U}$ contains all desired reflection coefficients as perturbations of the vanishing reflection coefficients in the background medium. Equation (14) can be used to obtain the linearized reflection/transmission coefficients for all possible types of incidence waves and arbitrarily anisotropic media.

Incident *P*-wave

Here, equation (14) is solved for an incident P-wave. Analogous approach can be used for an incident S-wave.

Let us consider a horizontal plane interface [the normal $\boldsymbol{n} = (0, 0, 1)$], and an incident P-wave propagating in the halfspace denoted as 1 and approaching the interface in the negative z-direction (Figure 1a). For simplicity, the incidence plane, defined by the normal $\boldsymbol{n}$ and the slowness vector of the incident P-wave, coincides with the [x, z] plane of the reference Cartesian coordinate system. Later on, the final formulas will be generalized for an arbitrary azimuth.

First, let us analyze the reflection/transmission problem for the background medium. The slowness vectors $\boldsymbol{p}^{0(N)}$ of all waves in the background medium ($N = 0, 1, 2, 3$ correspond to the incident wave and S_1, S_2 and P reflected waves, respectively; $N = 4, 5, 6$ correspond to S_1, S_2 and P transmitted waves, respectively), formally generated at the fictitious interface, can be written as

$$\begin{aligned} \boldsymbol{p}^{0(0)} = \boldsymbol{p}^{0(6)} &= (p_1^0, 0, p_3^{0P})^T, \\ \boldsymbol{p}^{0(1)} = \boldsymbol{p}^{0(2)} &= (p_1^0, 0, -p_3^{0S})^T, \\ \boldsymbol{p}^{0(3)} &= (p_1^0, 0, -p_3^{0P})^T, \\ \boldsymbol{p}^{0(4)} = \boldsymbol{p}^{0(5)} &= (p_1^0, 0, p_3^{0S})^T. \end{aligned} \tag{15}$$

According to Snell's law, the horizontal slowness $p_1^0 = \sin i/\alpha$ is constant for all waves. Vertical slownesses p_3^{0P} and p_3^{0S} satisfy the relations $p_3^{0P} = \cos i/\alpha$ and $p_3^{0S} = \cos j/\beta$. Here, α and β are the P- and S-wave velocities in the background medium, i is the P-wave incidence angle and j is the S-wave reflection angle. They are taken as the acute angles between the corresponding slowness vector and the normal $\boldsymbol{n}$.

The P-wave polarization vectors in the background medium are given simply as

$$\begin{aligned} \boldsymbol{g}^{0(0)} = \boldsymbol{g}^{0(6)} &= \alpha(p_1^0, 0, p_3^{0P})^T, \\ \boldsymbol{g}^{0(3)} &= \alpha(p_1^0, 0, -p_3^{0P})^T. \end{aligned} \tag{16}$$

The S-wave polarization vectors in an isotropic medium usually are projected onto the incidence [x, z] plane (SV-wave polarization) and the direction perpendicular to the plane (SH-wave polarization; see Figure 1a). However, Jech and Pšenčík (1989) showed that such a choice is no longer acceptable if the S-wave polarization vectors in a weakly anisotropic medium are to be found by means of small (linear) perturbations from the S-wave polarization vectors in the background isotropic medium. To minimize the perturbations, the chosen polarization vectors in the background isotropic medium must be rotated in the plane perpendicular to the corresponding S-wave slowness vector (the plane of rotation, see Figure 1b) by a certain *polarization angle* Φ.

Of course, the rotated polarization vectors are still mutually perpendicular and satisfy the Christoffel equation (7). Jech and Pšenčík (1989) also showed that, except for S-wave singular points, Φ is defined uniquely. An S-wave singular point is a slowness direction in which the slowness surfaces of the S_1- and S_2-waves intersect each other, and both waves propagate with the same phase velocity. Jech and Pšenčík (1989) and Pšenčík (1998) derived an explicit analytical expression for the polarization angle Φ as a function of the parameter perturbations δa_{ijkl} defined in equation (10). Unfortunately, the polarization angle Φ is not a linear function of δa_{ijkl}. This fact complicates the final approximations for PS-wave reflection coefficient and their application becomes more involved that that for PP-wave reflections.

For now, I assume that the polarization angle Φ is known and is positive in the counter-clockwise direction from the vector $\boldsymbol{g}^{SV}$ towards the vector $\boldsymbol{g}^{SH}$ (Figure 1b). Thus, $\boldsymbol{g}^{SV}$ and $\boldsymbol{g}^{SH}$ are still important reference polarizations representing, together with slowness vector $\boldsymbol{p}^{0(1)} = \boldsymbol{p}^{0(2)}$, the base vectors of a local right-handed Cartesian coordinate system that will be used later. In the incidence halfspace, the polarization angle Φ defines two reflected waves S_1^0 and S_2^0 in the background medium with the following polarization vectors (Figure 1b):

$$\begin{aligned} \boldsymbol{g}^{0(1)} &= (-\beta p_3^{0S} \cos\Phi, \sin\Phi, -\beta p_1^0 \cos\Phi)^T, \\ \boldsymbol{g}^{0(2)} &= (\beta p_3^{0S} \sin\Phi, \cos\Phi, \beta p_1^0 \sin\Phi)^T. \end{aligned} \tag{17}$$

Obviously, if $\Phi = 0$ (as in isotropic medium), S_1^0 reduces to the conventional SV-wave and S_2^0 to the SH-wave. As shown in Jech and Pšenčík (1989), the background polarization vectors (17) can be further perturbed to approximate the true polarization vectors in a weakly anisotropic medium (which in general do not lie in the [$\boldsymbol{g}^{0(1)}$, $\boldsymbol{g}^{0(2)}$] plane). These small (linear) perturbations $\delta\boldsymbol{g}^{(1)}$, $\delta\boldsymbol{g}^{(2)}$ [see equation (12)] define the reflected S_1 and S_2 waves in the weakly anisotropic medium.

Similarly, for the transmitted S-waves,

$$\begin{aligned} \boldsymbol{g}^{0(4)} &= (\beta p_3^{0S} \cos\Psi, \sin\Psi, -\beta p_1^0 \cos\Psi)^T, \\ \boldsymbol{g}^{0(5)} &= (-\beta p_3^{0S} \sin\Psi, \cos\Psi, \beta p_1^0 \sin\Psi)^T, \end{aligned} \tag{18}$$

where Ψ is the corresponding polarization angle.

Once the slowness vectors (15) and the polarization vectors (16), (17) and (18) have been defined, it is possible to create the background polarization-traction matrix $\hat{\mathbf{C}}^0$ as introduced in relations (13) using the velocities α, β, and the density ρ^0 for the background medium [equations (9) and (10)]. An explicit form of the matrix $\hat{\mathbf{C}}^0$, as well as its inverse $(\hat{\mathbf{C}}^0)^{-1}$, needed in equation (14), has been derived in Vavryčuk and Pšenčík (1998) and can be found in Appendix A.

For an incident P-wave, the background reflec-

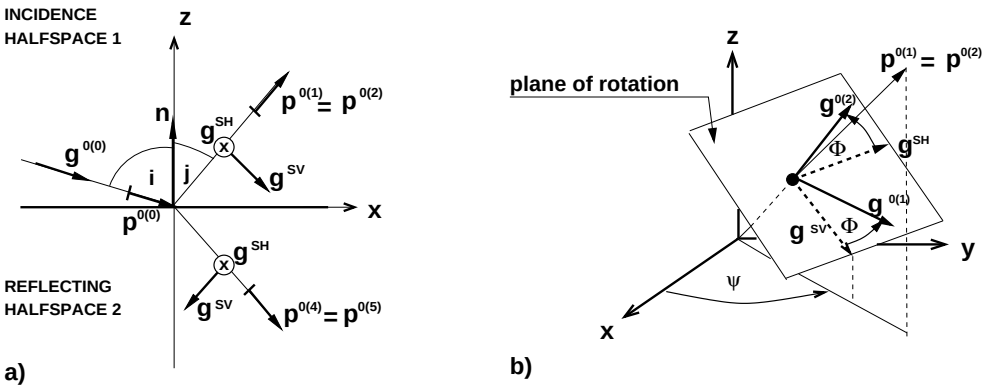

Figure 1. To the derivation of the reflection/transmission coefficients. 1a) conventions for the zero-azimuth reflection/transmission (in the plane [x, z]) in the background medium. Incidence plane is defined by the normal $\boldsymbol{n}$ and the background P-wave slowness vector $\boldsymbol{p}^{0(0)}$ (or the background S-wave slowness vectors $\boldsymbol{p}^{0(1)} = \boldsymbol{p}^{0(2)} = \boldsymbol{p}^{0(4)} = \boldsymbol{p}^{0(5)}$). The angles i and j represent the P-wave incidence and the S-wave reflection/transmission phase angles, respectively. Vector $\boldsymbol{g}^{0(0)}$ denotes the polarization vector of the incidence P-wave in the background medium, $\boldsymbol{g}^{SV}$ and $\boldsymbol{g}^{SH}$ are the reflected SV- and SH-wave polarization vectors in the background medium ($\boldsymbol{g}^{SH}$ points away from the reader, parallel to the y-axis). 1b) the positive azimuthal angle ψ (counted from the x-axis towards the y-axis) and the isotropic background S-wave polarization vectors $\boldsymbol{g}^{0(1)}$ and $\boldsymbol{g}^{0(2)}$ rotated in the plane perpendicular to the S-wave slowness vector $\boldsymbol{p}^{0(1)} = \boldsymbol{p}^{0(2)}$ (plane of rotation) by the polarization angle Φ with respect to the polarization vectors $\boldsymbol{g}^{SV}$ and $\boldsymbol{g}^{SH}$; see the text for details.

tion/transmission vector $\boldsymbol{U}^0$ is given by [equations (8) and (14)]:

$$\boldsymbol{U}^0 = (0, 0, 0, 0, 0, 1)^T. \tag{19}$$

This fact considerably simplifies the general equation (14), since only the 6th column of the perturbation matrix $\delta\hat{\mathbf{C}}$ [see equation (6)] has to be evaluated (together with the perturbation vector $\delta\boldsymbol{B}$). Thus, perturbations of the polarization and normalized traction vectors are required only for the incident and transmitted P-waves.

Finally, substituting equation (19) into (14) and using relations (6), (12) and (13) yields

$$\delta\boldsymbol{U} = (\hat{\mathbf{C}}^0)^{-1} \left(\delta g_1^{(6)} - \delta g_1^{(0)}, \delta g_2^{(6)} - \delta g_2^{(0)}, \delta g_3^{(6)} - \delta g_3^{(0)},\right.$$
$$\left.\delta X_1^{(6)} - \delta X_1^{(0)}, \delta X_2^{(6)} - \delta X_2^{(0)}, \delta X_3^{(6)} - \delta X_3^{(0)}\right)^T. \tag{20}$$

The differences $\delta g_i^{(6)} - \delta g_i^{(0)}$ between the perturbed polarization vectors and $\delta X_i^{(6)} - \delta X_i^{(0)}$ between the normalized traction vectors are given in Appendix A [equations (A3) and (A8)].

General form of the approximate PS-wave reflection coefficients

Equation (20) allows us to evaluate all reflection/transmission coefficients corresponding to the incidence P-wave (R_{PS_1}, R_{PS_2}, R_{PP}, T_{PS_1}, T_{PS_2} and T_{PP}). Pšenčík and Vavryčuk (1998) obtained relatively simple expressions for both P-wave reflection and transmission coefficients R_{PP} and T_{PP} valid for arbitrarily anisotropic media. Since their equations are linear in the elastic parameters, they can be conveniently applied in linear inversion.

Derivation of R_{PS_1} and R_{PS_2}, however, is somewhat more complicated. To obtain the needed approximations, the first two rows of the matrix $(\hat{\mathbf{C}}^0)^{-1}$ are to be used [see equations (8), (13), (19) and (20)]. They contain the polarization angle Φ introduced above (Figure 1b). It can be shown that the angle Φ is not small even for weak anisotropy and thus can be neither neglected nor linearized. Notice that the angle Φ does not appear in the derivations of R_{PP} and T_{PP} coefficients. Also, the terms $\delta g_2^{(6)} - \delta g_2^{(0)}$ and $\delta X_2^{(6)} - \delta X_2^{(0)}$ in equation (20) are not necessary for deriving R_{PP} and T_{PP} approximations due to the zero elements in the 3rd and 6th rows of the matrix $(\hat{\mathbf{C}}^0)^{-1}$.

To proceed with the derivation, the polarization angle Φ is considered as known for now and will be discussed later on. First, I derive the reflection coefficient of the PS_1-wave (R_{PS_1}) using the first row of the matrix $(\hat{\mathbf{C}}^0)^{-1}$. This coefficient is uniquely defined by the polarization angle Φ, equations (17) and the convention introduced in Figure 1b. The second coefficient R_{PS_2}, determined by the second row of the matrix $(\hat{\mathbf{C}}^0)^{-1}$, is easy to obtain directly from the coefficient R_{PS_1} by the substitutions $\cos\Phi \to -\sin\Phi$ and $\sin\Phi \to \cos\Phi$, since this is the only difference between the rows 1 and 2 of the matrix $(\hat{\mathbf{C}}^0)^{-1}$.

Substituting equations (A2), (A3) and (A8) into (20), and evaluating all necessary quantities from equations (A5), (A7) and (A9) [together with (10), (15), (16) and (A6)], I obtained a general formula for the R_{PS_1}

reflection coefficient valid in the incidence plane [x, z]. The tedious algebra has been done partly by hand and partly using the symbolic software Mathematica. The final equation can be formally written as

$$\begin{aligned} R_{PS_1} \quad = \quad & f\left(\alpha, \beta, \rho^0, i, j, \Phi, \Delta A_{11}, \Delta A_{13}, \Delta A_{14}, \right. \\ & \Delta A_{15}, \Delta A_{16}, \Delta A_{33}, \Delta A_{34}, \Delta A_{35}, \\ & \left. \Delta A_{36}, \Delta A_{45}, \Delta A_{55}, \Delta A_{56}\right), \end{aligned} \tag{21}$$

where the parameters $\Delta A_{ij} = A_{ij}^{(2)} - A_{ij}^{(1)}$ represent the contrasts in the density normalized elastic medium parameters a_{klmn} across the interface, written in the well-known Voigt convention [see equation (A6)].

Formula (21) can be generalized for an arbitrary orientation (azimuth) of the incidence plane with respect to the [x, z] plane of the reference coordinate system. Taking into account the convention introduced in Figure 1b, the elements ΔA_{ij} can be expressed in the coordinate system rotated with respect to the reference coordinate system around the z-axis by an angle ψ as

$$\Delta A_{ij} = f_t\left(\psi, \Delta A'_{kl}\right), \tag{22}$$

where f_t represents the transformation function and $\Delta A'_{kl}$ are the elastic medium parameters in the reference coordinate system. Explicit expressions for f_t can be found in Appendix B. Substituting transformation (22) into equation (21), and using ΔA_{ij} instead of $\Delta A'_{ij}$, leads to the final, most general expression for the weak-contrast, weak-anisotropy reflection coefficient R_{PS_1}. I performed this substitution using Mathematica and obtained an expression that can be written in the following compact form:

$$R_{PS_1} = R_{PSV} \cdot \cos\Phi + R_{PSH} \cdot \sin\Phi. \tag{23}$$

Terms R_{PSV} and R_{PSH} depend on the incidence angle i, reflection angle j and azimuthal angle ψ, and are linear functions of the contrasts in the elastic parameters ΔA_{ij}. Explicit expressions for R_{PSV} and R_{PSH} are listed in Appendix B and will be described later in more detail. As discussed above, it is straightforward to write an analogous expression for the other reflection coefficient,

$$R_{PS_2} = -R_{PSV} \cdot \sin\Phi + R_{PSH} \cdot \cos\Phi. \tag{24}$$

It should be emphasized that in the weak-anisotropy approximation the coefficients (23) and (24) determine the amplitudes of the PS_1- and PS_2-reflected waves polarized in the vicinity of the $\boldsymbol{g}^{0(1)}$ and $\boldsymbol{g}^{0(2)}$ directions, respectively (see Figure 1b). Thus the true amplitudes can be approximated as

$$\begin{aligned} U^{(1)}\boldsymbol{g}^{(1)} \quad &\approx \quad \boldsymbol{g}^{0(1)} \cdot R_{PS_1} \cdot U^{(0)}, \\ U^{(2)}\boldsymbol{g}^{(2)} \quad &\approx \quad \boldsymbol{g}^{0(2)} \cdot R_{PS_2} \cdot U^{(0)}, \end{aligned} \tag{25}$$

where $U^{(0,1,2)}$ and $\boldsymbol{g}^{(1,2)}$ are defined in equation (1). The perturbations of the true polarization vectors [equations (12)] from the background polarizations $\boldsymbol{g}^{0(1)}$ and $\boldsymbol{g}^{0(2)}$ are neglected in equation (25) since they contribute to the nonlinear terms only. This important concept will be used later to account for the polarization angle Φ.

Clearly, coefficients (23) and (24) are not linear functions of the medium parameters A_{ij} due to the nonlinearity of the angle Φ. Therefore, the term "*linearized reflection coefficient*", commonly used for P-wave approximations, cannot be strictly applied in this case. Another difference from the P-wave coefficients is that the coefficients (23) and (24) contain all 21 contrast parameters ΔA_{ij} (see Appendix B). As shown in Vavryčuk and Pšenčík (1998), R_{PP} approximations contain only 13 medium parameters in the most general case (triclinic symmetry).

Another interesting (but not surprising) observation, which can be made from equations (23), (24) and (B3)-(B5), is that even a vertically incident P-wave can generate reflected S-wave at a horizontal interface. The quantities largely responsible for such a reflection, in the first-order approximation, are the elastic parameters ΔA_{34} and ΔA_{35} (notice that neither incidence plane nor the g^{SV} and g^{SH} polarizations are uniquely defined for such a case). Of course, in isotropic media A_{34} and A_{35} vanish and the conversion at normal incidence does not exist. This is also true for a horizontal interface between two anisotropic halfspaces with a horizontal symmetry plane. Similarly, medium parameter contrasts mostly responsible for atypical incidence-plane P-SH reflections (i.e. the reflected S-wave is polarized perpendicular to the incidence plane) can be identified. For instance, at zero azimuth, the non-zero contrasts ΔA_{14}, ΔA_{16}, ΔA_{34}, ΔA_{36}, ΔA_{45} and ΔA_{56} would generate such a reflection. It will be shown later that this reflection can occur, for example, at the isotropic/HTI or VTI/HTI interface.

R_{PS_1} and R_{PS_2} coefficients for orthorhombic media

Here, general equations (23) and (24) are specified for an interface between two orthorhombic media, using the Thomsen-type parameterization of Tsvankin (1997b). Assuming orthorhombic or higher symmetry leads to a significant simplification of the general equations (23) and (24). The resulting expressions can be easily adopted for an interface separating any two of the following media: isotropic, VTI, HTI and orthorhombic.

The first step is to choose the background velocities α and β and the density ρ^0. Following Banik (1987) and others, the background values are defined as the average

of the corresponding quantities in both halfspaces,

$$\begin{aligned} \alpha &\equiv \bar{\alpha} \equiv \frac{1}{2}(\alpha^{(1)} + \alpha^{(2)}), \\ \beta &\equiv \bar{\beta} \equiv \frac{1}{2}(\beta^{(1)} + \beta^{(2)}), \\ \rho^0 &\equiv \bar{\rho} \equiv \frac{1}{2}(\rho^{(1)} + \rho^{(2)}). \end{aligned} \tag{26}$$

It is not clear, however, what velocities in (26) should be averaged for anisotropic media. Any particular choice results in slightly different forms of the final reflection coefficients. Motivated by this fact, Pšenčík and Martins (1999) derived formulas for the coefficients R_{PP} and T_{PP} with arbitrary values of the isotropic background velocities. They proved that different background velocities influence the accuracy of the approximations and they suggested to improve the accuracy in different ranges of incidence angles by varying α and β. It has been shown (Pšenčík and Martins, 1999), however, that for small incidence angles, the choice of vertical velocities is the most appropriate. For large angles, first-order reflection/transmission coefficients usually lose their accuracy due to neglected higher-order terms.

The choice of vertical velocity is non-unique for S-waves since in anisotropic media there are two vertically propagating S-waves with different velocities. My numerical tests for the approximate R_{PP} coefficients for different models suggest to choose the S-wave background velocity anywhere between the two vertical velocities of S_1- and S_2-waves. The resulting formulas slightly differ in accuracy, but these differences are often negligible, especially for small and moderate incidence angles. Therefore, the background velocities (26) are defined as the average of the following velocities of the two halfspaces:

$$\alpha^{(I)} = \sqrt{A_{33}^{(I)}}, \qquad \beta^{(I)} = \sqrt{A_{55}^{(I)}}, \qquad I = 1, 2. \tag{27}$$

The second important step in the derivation is the choice of medium parameterization. Tsvankin (1997b) introduced an efficient way of parameterizing orthorhombic media by generalizing Thomsen's notation for VTI media (Thomsen, 1986). An almost identical parameterization proved to be useful for the approximate reflection coefficient as well. Without any changes I adopt the following anisotropic parameters (Tsvankin, 1997b):

$$\epsilon_I^{(1)} \equiv \frac{A_{22}^{(I)} - A_{33}^{(I)}}{2A_{33}^{(I)}}, \tag{28}$$

$$\epsilon_I^{(2)} \equiv \frac{A_{11}^{(I)} - A_{33}^{(I)}}{2A_{33}^{(I)}}, \tag{29}$$

$$\gamma_I^{(S)} \equiv \frac{A_{44}^{(I)} - A_{55}^{(I)}}{2A_{55}^{(I)}}, \tag{30}$$

where I=1,2 represent the incidence and reflecting halfspaces, respectively. Further, I introduce three other parameters,

$$\tilde{\delta}_I^{(1)} \equiv \frac{A_{23}^{(I)} + 2A_{44}^{(I)} - A_{33}^{(I)}}{A_{33}^{(I)}}, \tag{31}$$

$$\tilde{\delta}_I^{(2)} \equiv \frac{A_{13}^{(I)} + 2A_{55}^{(I)} - A_{33}^{(I)}}{A_{33}^{(I)}}, \tag{32}$$

$$\tilde{\delta}_I^{(3)} \equiv \frac{A_{12}^{(I)} + 2A_{66}^{(I)} - A_{11}^{(I)}}{A_{11}^{(I)}}. \tag{33}$$

They differ from those in Tsvankin (1997b) defined as

$$\delta_I^{(1)} \equiv \frac{(A_{23}^{(I)} + A_{44}^{(I)})^2 - (A_{33}^{(I)} - A_{44}^{(I)})^2}{2A_{33}^{(I)}(A_{33}^{(I)} - A_{44}^{(I)})}, \tag{34}$$

$$\delta_I^{(2)} \equiv \frac{(A_{13}^{(I)} + A_{55}^{(I)})^2 - (A_{33}^{(I)} - A_{55}^{(I)})^2}{2A_{33}^{(I)}(A_{33}^{(I)} - A_{55}^{(I)})}, \tag{35}$$

$$\delta_I^{(3)} \equiv \frac{(A_{12}^{(I)} + A_{66}^{(I)})^2 - (A_{11}^{(I)} - A_{66}^{(I)})^2}{2A_{11}^{(I)}(A_{11}^{(I)} - A_{66}^{(I)})}. \tag{36}$$

It can be shown (Sayers, 1994) that the anisotropic parameters (31), (32) and (33) represent linearized forms of the "exact" parameters (34), (35) and (36), respectively. Therefore, for weak anisotropy, both sets of parameters are numerically close to each other (Pšenčík and Martins, 1999). This suggests that despite the fact that the derivation of R_{PS_1} and R_{PS_2} must be carried out using the parameters (31)-(33), both sets of parameters can be used in the final formulas without a significant impact on accuracy. This has been confirmed by Pšenčík and Martins (1999). Numerical tests I have done for the R_{PP} approximations showed only negligible differences (neither of these sets proved to be superior in general). For strongly anisotropic media, where both parameter sets would produce different results, the approximations are not sufficiently accurate anyway. In practice, it may be better to use the parameters (34)-(36) since they determine the exact V_{nmo} velocity. A generalized form of the parameterization (28)-(33) has been introduced by Pšenčík and Gajewski (1998) for arbitrarily weakly anisotropic media.

As shown bellow, the six anisotropic parameters (28)-(33) [together with the background parameters (26)] are sufficient for derivation of R_{PS_1}, R_{PS_2} coefficients, whereas an orthorhombic medium is fully described by seven anisotropic parameters (plus two vertical velocities). Tsvankin's (1997b) notation also contains two parameters γ_1 and γ_2. The approximations of R_{PS_1}, R_{PS_2}, however, are more sensitive to the difference $\gamma_1 - \gamma_2$ than to the parameters γ_1 and γ_2 separately. Thus, the number of parameters can be reduced. Notice that the parameter $\gamma^{(S)}$ [definition (30)] is equal to the difference $\gamma_1 - \gamma_2$ in the weak-anisotropy approximation.

Finally, we can complete the derivation of R_{PS_1},

R_{PS_2}. Assuming that one of the symmetry planes of both orthorhombic halfspaces is horizontal and that the vertical symmetry planes of the reflecting orthorhombic halfspace are rotated with respect to the vertical planes of the incidence orthorhombic halfspace by an angle denoted as κ, the following elastic parameters vanish:

$$A_{14}^{(1)} = A_{15}^{(1)} = A_{16}^{(1)} = A_{24}^{(1)} = A_{25}^{(1)} = A_{26}^{(1)} = A_{34}^{(1)} = \\ = A_{35}^{(1)} = A_{36}^{(1)} = A_{45}^{(1)} = A_{46}^{(1)} = A_{56}^{(1)} = 0, \qquad (37)$$

$$A_{14}^{(2)} = A_{15}^{(2)} = A_{24}^{(2)} = A_{25}^{(2)} = A_{34}^{(2)} = A_{35}^{(2)} = A_{46}^{(2)} = \\ = A_{56}^{(2)} = 0.$$

Substituting relations (37), together with the definitions (26)-(33), into equations (B3), (B4) and (B5), and further linearizing in the anisotropic parameters (28)-(33) yields the final formulas for the PS-wave reflection coefficients:

$$\begin{aligned} R_{PS_1} &= R_{PSV}\cos\Phi + R_{PSH}\sin\Phi, \qquad (38)\\ R_{PS_2} &= -R_{PSV}\sin\Phi + R_{PSH}\cos\Phi. \end{aligned}$$

Here,

$$\begin{aligned} R_{PSV} &= V_1\cos i\sin i + V_2\frac{\sin i}{\cos j} + V_3\cos i\sin^3 i \\ &\quad + V_4\frac{\sin^3 i}{\cos j} + V_5\frac{\sin^5 i}{\cos j}, \qquad (39)\\ R_{PSH} &= H_1\sin i + H_2\frac{\cos i\sin i}{\cos j} + H_3\sin^3 i \\ &\quad + H_4\frac{\cos i\sin^3 i}{\cos j}, \end{aligned}$$

where i, j are the incidence and reflection phase angles, respectively. Coefficients V_l and H_l are functions of the medium parameters [equations (26)-(36)], the azimuthal angle ψ and the angle κ. The explicit expressions for V_l and H_l are given in Appendix C [equations (C1) and (C2)]. Finally, the polarization angle Φ should be evaluated in equations (38). The angle Φ can be computed theoretically as long as all anisotropic parameters of the incidence medium are known. Corresponding equations are derived in Appendix D. As discussed later on, however, the polarization angle Φ can be also determined directly from data. This is important in practical applications since the knowledge of the medium parameters is not necessary.

R_{PS_1} and R_{PS_2} coefficients for isotropic, VTI, HTI and orthorhombic halfspaces

Since isotropic, VTI and HTI media are special cases of the orthorhombic medium, R_{PS_1} and R_{PS_2} coefficients derived in the previous section can be immediately used for an interface separating any of two of the following halfspaces: isotropic, VTI, HTI or orthorhombic. In order to do so, only the anisotropic parameters in V_l and H_l [equations (39)] have to be adapted for a specific model as shown by Tsvankin (1997b). The necessary anisotropic parameters used for VTI media are defined as

$$\begin{aligned} \epsilon &\equiv \frac{A_{11}-A_{33}}{2A_{33}},\\ \delta &\equiv \frac{(A_{13}+A_{55})^2-(A_{33}-A_{55})^2}{2A_{33}(A_{33}-A_{55})}, \end{aligned}$$

and for HTI media,

$$\begin{aligned} \epsilon^{(V)} &\equiv \frac{A_{11}-A_{33}}{2A_{33}}, \qquad (40)\\ \delta^{(V)} &\equiv \frac{(A_{13}+A_{55})^2-(A_{33}-A_{55})^2}{2A_{33}(A_{33}-A_{55})},\\ \gamma &\equiv \frac{A_{44}-A_{66}}{2A_{66}}. \end{aligned}$$

For a more detailed discussion of the anisotropic coefficients for VTI and HTI media, see Tsvankin (1996, 1997a) and Thomsen (1986). Of course, for isotropic media, the parameters vanish in V_l , and $H_l = 0$ for all $l = 1, ..., 4$, see equations (C1) and (C2).

orthorhombic	HTI	VTI
$\epsilon^{(1)}$	0	ϵ
$\epsilon^{(2)}$	$\epsilon^{(V)}$	ϵ
$\gamma^{(S)}$	γ	0
$\delta^{(1)}$	0	δ
$\delta^{(2)}$	$\delta^{(V)}$	δ
$\delta^{(3)}$	$\delta^{(V)} - 2\epsilon^{(V)}$	0

Table 1. Conversion table of the anisotropy parameters (weak-anisotropy approximation) for VTI, HTI and orthorhombic media. VTI and HTI parameters are defined by equations (40). The symmetry axis of the HTI medium points in the x-direction.

Table 1 shows the conversion key. For example, if the upper medium is VTI, all parameters with the subscript 1 in equations (C1) and (C2) have to be replaced by the corresponding VTI parameters listed in the third column of Table 1.

It should be also pointed out that the polarization angle Φ in equations (38) is easily determined, assuming isotropic, VTI or HTI symmetry, as shown in Appendix D.

Discussion

Here, I discuss the general expressions (23), (24) and (38) for R_{PS_1} and R_{PS_2} and compare them with those

obtained by Rüger (1996). Then, I describe the components R_{PSV} and R_{PSH} defined by equations (39).

Comparison of R_{PS_1} and R_{PS_2} with the results of Rüger (1996)

The generality of expressions (23), (24) and (38) represents, of course, the fundamental difference from the expressions obtained by Rüger (1996) for the symmetry planes of HTI media. However, the derivation described in this paper is based on the same principle of linearization of the general equation (4), except that the linearization is performed for a different set of medium parameters defined for general anisotropy. Therefore, the resulting expressions should be analogous to those derived by Rüger (1996) for the isotropy and symmetry-axis planes of HTI media (assuming that the symmetry axes of both HTI halfspaces are aligned). Indeed, expressions (38) specified for an HTI/HTI interface (using Table 1), for the azimuthal angles $\psi = 0°$ and $\psi = 90°$, and the symmetry-plane rotation angle $\kappa = 0$ [equations (C1)-(C2)], reduce to Rüger's expressions (see Rüger, 1996, Appendix D). Notice, that for the azimuths $\psi = 0°$ and $\psi = 90°$, the polarization angle Φ is equal to ψ (i.e. $0°$ and $90°$, respectively).

Strictly speaking, the analogy is not exact, since expressions (38) include the linear parameters (31)-(33) rather than the nonlinear parameters (34)-(36) contained in Rüger's expressions. However, as discussed above, in weakly anisotropic media these two sets of parameters can be formally interchanged without a strong impact on accuracy.

Another difference of the approach described here from that by Rüger (1996) is the possibility to choose an arbitrary isotropic background [see the discussion related to definitions (26) and (27)]. In my opinion, the choice of the arbitrary isotropic background is important for more complicated models, such as those with arbitrary orientation of symmetry axes (for TI media) or symmetry planes (for orthorhombic media). Also, for such models it is more efficient to change the parameterization defined by (28)-(33), see Pšenčík and Martins (1999).

R_{PS_1} and R_{PS_2} coefficients vs. R_{PP} coefficient

General equations (23) and (24), as well as equation (38), indicate that practical application of R_{PS} reflection coefficients will be more problematic than that of R_{PP} coefficients.

The first apparent complication comes from the fact that the final equations (23), (24) and (38) include both the incidence and reflection phase angles i and j related by Snell's law in anisotropic media. This inconvenience, however, can be easily overcome by using the weak-contrast, weak-anisotropy assumption.

Since the factor $(\cos j)^{-1}$ in equations (39) is always multiplied by the contrasts in one of the anisotropic parameters [equations (C1)-(C2); see also equations (B3), (B4) and (B5) for general case], it is possible to use purely isotropic Snell's law. The errors associated with such an approximation are of second order, and thus can be neglected in the linearized approximation. Therefore,

$$\frac{1}{\cos j} \approx \frac{1}{\sqrt{1 - \frac{\bar{\beta}^2}{\bar{\alpha}^2}\sin^2 i}} \approx 1 + \frac{1}{2}\frac{\bar{\beta}^2}{\bar{\alpha}^2}\sin^2 i, \tag{41}$$

where $\bar{\alpha}$ and $\bar{\beta}$ are defined in (26) and (27). In the derivation of (41), an additional assumption of a small $\sin^2 i$ has been used. Numerical tests show that such an assumption works well for a wide range of $\bar{\alpha}/\bar{\beta}$ ratios, and for incidence angles corresponding to the offset to depth ratios conventionally used in AVO. Moreover, similarly to R_{PP}, the approximations for R_{PS_1} and R_{PS_2} lose their accuracy for larger incidence angles anyway. The same approach can be used to express the coefficients R_{PS_1} and R_{PS_2} in terms of the reflection angle j or horizontal slowness p_1, which may be convenient for some applications. Equation (41) can be directly substituted into relations (B3) or (39).

The second complication with R_{PS_1} and R_{PS_2} is more troublesome. As mentioned above, the coefficients (23), (24) and (38) are not purely linear functions of the medium parameters due to the nonlinearity of the polarization angle Φ. Hence, the influence of the polarization angle Φ should be eliminated in R_{PS_1} and R_{PS_2} before further analysis.

Such an elimination is straightforward if the incidence medium is either isotropic or VTI, and $\cos\Phi = 1$ and $\sin\Phi = 0$. Also, for HTI media it is possible to use relations (D6), if the azimuth (the angle between the incidence and symmetry-axis plane) is known. In principle, this should not represent a significant complication since the symmetry-axis plane (as well as isotropy plane) of HTI media can be identified using the travel times and polarizations of S-waves or by analysis of the P-wave NMO ellipse (Grechka and Tsvankin, 1998).

For an orthorhombic incidence halfspace, however, the situation is more complicated. The relations (D1)-(D5) can be applied only if all nine medium parameters of the halfspace are known, which is not usually the case. Therefore, a different method must be used to account for the polarization angle Φ.

It is convenient to formally introduce the PS-wave reflection coefficient vector as

$$\boldsymbol{R}_{PS} = (R_{PS_1}, R_{PS_2}), \tag{42}$$

where R_{PS_1} and R_{PS_2} are defined by equations (23) and (24). As follows from equations (25), the reflection coefficient vector (42) is specified in the coordinate system $\boldsymbol{g}^{0(1)} - \boldsymbol{g}^{0(2)}$ and approximates the exact reflection coefficient vector $\boldsymbol{R}_{PS}^{ext} = (R_{PS_1}^{ext}, R_{PS_2}^{exc})$ specified in the coordinate system $\boldsymbol{g}^{(1)ext} - \boldsymbol{g}^{(2)ext}$ ($R_{PS_1}^{ext}$ and $R_{PS_2}^{exc}$ are the exact PS-wave reflection coefficients corresponding to the exact S-wave polarization vectors $\boldsymbol{g}^{(1)ext}$ and $\boldsymbol{g}^{(2)ext}$, respectively). The same reflection coefficient vector (42) can be also written in the coordinate system $\boldsymbol{g}^{SV} - \boldsymbol{g}^{SH}$ (see Figure 1b) as

$$\boldsymbol{R}'_{PS} = (R_{PSV}, R_{PSH}), \tag{43}$$

where R_{PSV} and R_{PSH} are introduced in equations (23) and (24). The representation (43) of the reflection coefficient vector is independent of the polarization angle Φ and is purely linear in the elastic parameters. Thus, the desired transformation to be found is

$$\boldsymbol{R}_{PS}^{ext} \approx \boldsymbol{R}_{PS} \rightarrow \boldsymbol{R}'_{PS} \ . \tag{44}$$

The transformation (44) consists only of the projection of the vector $\boldsymbol{R}_{PS}^{ext}$ (extracted from data) onto the $\boldsymbol{g}^{SV}$ and $\boldsymbol{g}^{SH}$ directions, which gives the desired components R_{PSV} and R_{PSH}. The directions $\boldsymbol{g}^{SV}$ and $\boldsymbol{g}^{SH}$ can be determined from the background slowness vector (see Figure 1b) which should be close to the corresponding isotropic S-wave propagation direction. Thus, in weakly anisotropic media, this direction can be chosen in several ways. For example, the direction of the slowness vector can be simply chosen as perpendicular to the both S-wave polarization vectors previously extracted from data. Another possibility is to estimate the direction of the background isotropic slowness vector from the known azimuthal and incidence phase angles using isotropic Snell's law [similarly to the derivation of equation (41)].

The transformation (44) is fully general, applicable on any weakly anisotropic halfspaces. Of course, for strong anisotropy, the transformation will fail, but approximations (23) and (24) are designed for weak anisotropy anyway. Moreover, the transformation (44) does not require any additional operation applied on data; polarization analysis have to be carried out in any case in order to properly recover the PS-wave amplitudes.

A similar transformation can be used if only one of the R_{PS_1} and R_{PS_2} reflection coefficients is known. However, the directions of both S_1- and S_2-wave polarizations should still be identified. Then, the polarization angle Φ can be estimated directly as an angle between the $\boldsymbol{g}^{(1)ext}$ and $\boldsymbol{g}^{SV}$ polarization vectors. Without the complementary PS-wave reflection coefficient, however, it is impossible to find the R_{PSV} and R_{PSH} components. They must be analyzed together, as in relation (23) or (24).

Finally, one more difference between applications of the PS- and PP-wave reflection coefficients should be emphasized. As already pointed out before, S-wave singularities in anisotropic media cause problems also for PS-wave reflection coefficients. For an orthorhombic incidence halfspace, the approximations (23) and (24) generally suffer from numerical instability due to ambiguously determined polarization angle Φ at the S-wave singular points. For isotropic, VTI and HTI incidence media, this instability is overcome by a formal separation of the S_1- and S_2-waves. Nevertheless, plane PS-wave reflection coefficients generally fail to represent amplitude signatures sufficiently well near S-wave singularities due to the complicated character of the wave field in those regions.

R_{PSV} and R_{PSH} components

As discussed in the previous section, estimates of $\sin\Phi$ and $\cos\Phi$ factors allow us to analyze equations (24), (25) or (38) for the coefficient R_{PS_1} or R_{PS_2} separately. It is more beneficial, however, to use them jointly in order to extract the individual linear components R_{PSV} and R_{PSH}. The components R_{PSV} and R_{PSH} can then be treated in a similar fashion as R_{PP} reflection coefficients discussed previously in the literature. It can be also shown that both R_{PSV} and R_{PSH} contain the same anisotropic medium parameters, but different angular dependencies. Therefore, their joint inversion may provide a more stable solution.

In addition to the anisotropic parameters, R_{PSV} also contains the isotropic contrast parameters $\Delta\rho/\bar{\rho}$ and $\Delta\beta/\bar{\beta}$. These parameters can be either eliminated by subtraction of two R_{PSV} components for two different azimuths, or retained and included in the inversion process. Notice that the R_{PSH} component contains no isotropic contrast parameters at all because there is only one non-zero reflection coefficient $R_{PS_1} = R_{PSV}$ in isotropic media [see equations (C1)-(C2), and equations (38) for $\Phi = 0°$]. Similarly, analysis of equations (39), (C1) and (C2) shows that only one non-zero coefficient (R_{PSV}) exists for isotropic/VTI, VTI/isotropic and VTI/VTI interfaces. All other interfaces generate both PS_1 and PS_2 non-zero reflections, although not necessarily for all azimuths.

As an example, consider the components R_{PSV} and R_{PSH} for an interface between two orthorhombic media. They contain the following 14 parameters [see (39), (C1) and (C2)] : $\Delta\rho/\bar{\rho}$, $\Delta\beta/\bar{\beta}$, $\gamma_1^{(S)}$, $\gamma_2^{(S)}$, $\epsilon_1^{(1)}$, $\epsilon_2^{(1)}$, $\epsilon_1^{(2)}$, $\epsilon_2^{(2)}$, $\delta_1^{(1)}$, $\delta_2^{(1)}$, $\delta_1^{(2)}$, $\delta_2^{(2)}$, $\delta_1^{(3)}$ and $\delta_2^{(3)}$. Notice that there is no contrast parameter $\Delta\alpha/\bar{\alpha}$ in this set, which always ap-

pears in P-wave reflection coefficients. Theoretically, the components R_{PSV} and R_{PSH} obtained for 7 different pairs $[i,\ \psi]$ are sufficient to invert for all the parameters. Of course, the pairs should cover a reasonably large incidence angle range and azimuths from 0° to 90° in order to obtain stable results (of course, this simplistic consideration assumes no errors in data or the R_{PSV} and R_{PSH} approximations, which is never true in practice). Clearly, different anisotropic parameters control R_{PSV} and R_{PSH} components in different ranges of azimuthal angles. If the symmetry planes of the incidence and reflecting orthorhombic halfspaces have close azimuths [see the angle κ in equations (C1) and (C2)], then only the contrasts of the medium parameters ($\Delta\rho/\bar{\rho}$, $\Delta\beta/\bar{\beta}$, $\Delta\gamma^{(S)}$, $\Delta\epsilon^{(1)}$, $\Delta\epsilon^{(2)}$, $\Delta\delta^{(1)}$, $\Delta\delta^{(2)}$, $\Delta\delta^{(3)}$) can be recovered.

Finally, as for the R_{PP} approximations, numerical accuracy of R_{PSV} and R_{PSH} components generally decreases with increasing incidence angle i. Therefore, the medium parameters inverted using large-angle terms may contain large errors. Taking this into account, the inversion for the parameters $\gamma^{(S)}$, $\delta^{(1)}$ and $\delta^{(2)}$ will certainly provide more reliable results than that for the parameters $\delta^{(3)}$, $\epsilon^{(1)}$ and $\epsilon^{(2)}$. Also, for weakly anisotropic halfspaces the component R_{PSH} is expected to be small and thus less stable than the component R_{PSV}.

R_{PSV} and R_{PSH} approximations for small incidence angles

In practical AVO analysis, one often uses reflection coefficients for relatively small incidence angles. Therefore, it is useful to simplify the components R_{PSV} and R_{PSH} from equations (39) by keeping only angular terms corresponding to small incidence angles.

Such a simplification is also justified by the fact that the approximations for the reflection coefficients (both PP and PS) generally lose accuracy at large incidence angles. This might be surprising since no assumption of small incidence angles has been used in the original derivation [an exception is equation (41) which is employed later in the derivation]. The loss of accuracy for large incidence angles has two main reasons. First, the terms associated with higher incidence angles contain increasing number of nonlinear factors (i.e. higher powers of the elastic parameters) and, eventually, linear factors may vanish from such terms completely. Thus, by neglecting all nonlinear factors we reduce the accuracy of the terms corresponding to higher incidence angles and, of course, that of the whole reflection coefficient. The second reason for loosing the accuracy, applicable on anisotropic media only, is the choice of the background velocities $\bar{\alpha}$ and $\bar{\beta}$ [see discussion of equations (26) and (27)] that have been selected as the vertical velocities.

To obtain small-angle approximations of R_{PSV} and R_{PSH}, the second and higher powers of $\sin i$ in equations (39) are neglected. Using expressions (C1) and (C2) and relation (41), we arrive at

$$
\begin{aligned}
R_{PSV} \;=\; & \left\{ -\frac{1+2g}{2}\frac{\Delta\rho}{\bar{\rho}} - 2g\frac{\Delta\beta}{\bar{\beta}} \right. \\
& + \frac{1}{2(1+g)}\delta_2^{(2)}\cos^2(\psi-\kappa) \\
& + \left[\frac{1}{2(1+g)}\delta_2^{(1)} - 2g\,\gamma_2^{(S)}\right]\sin^2(\psi-\kappa) \\
& - \frac{1}{2(1+g)}\delta_1^{(2)}\cos^2\psi \\
& \left. - \left[\frac{1}{2(1+g)}\delta_1^{(1)} - 2g\,\gamma_1^{(S)}\right]\sin^2\psi \right\}\sin i, \\
R_{PSH} \;=\; & \left\{ \left[\frac{1}{4(1+g)}(\delta_2^{(2)} - \delta_2^{(1)}) \right.\right. \\
& \left. + g\,\gamma_2^{(S)}\right]\sin 2(\psi-\kappa) \\
& - \left[\frac{1}{4(1+g)}(\delta_1^{(2)} - \delta_1^{(1)}) \right. \\
& \left.\left. + g\,\gamma_1^{(S)}\right]\sin 2\psi \right\}\sin i,
\end{aligned}
\qquad (45)
$$

where g represents the background velocity ratio $g \equiv \bar{\beta}/\bar{\alpha}$.

Equations (45) work well up to incidence angles 15°-20°. In order to improve the accuracy for larger angles, additional terms with $\sin^3 i$ and $\cos i \sin^3 i$ factors would have to be included. Unfortunately, this would no longer lead to a significant simplification, as clearly seen from equations (39), (C1) and (C2).

In analogy with the PP-wave reflection, equations (45) represent so called PS-wave AVO gradients. Notice that the PS-wave AVO gradients are associated with the term $\sin i$, whereas the PP-wave AVO gradient corresponds to $\sin^2 i$. The PS-wave AVO gradients can be extracted from data by recovering the linear trends on the plots $R_{PSV}(\sin i)$ and $R_{PSH}(\sin i)$. The AVO gradients can be used for fast rough estimates of the medium parameters as well as for a more sophisticated linear inversion of reflection coefficients. Joint inversion of the PP- and PS-wave AVO gradients can provide estimates of the parameters $\delta_{1,2}^{(1)}$, $\delta_{1,2}^{(2)}$ and $\gamma_{1,2}^{(S)}$ (assuming non-zero angle κ). Such an inversion cannot be carried out using R_{PP} approximations only since the corresponding expressions do not allow one to separate $\delta_{1,2}^{(1)}$ from $\gamma_{1,2}^{(S)}$ (see Pšenčík and Martins, 1999). As expected, equations (45) also verify that approximate small-incidence-angle PS reflections are not dependent on the parameters $\epsilon^{(1)}$, $\epsilon^{(2)}$ and $\delta^{(3)}$. The same is true for the reflection coeffi-

cient R_{PP}, as shown by Vavryčuk and Pšenčík (1998).

Numerical examples

Accuracy of the approximations (38) and (39) was tested on several anisotropic models. Most of the models here represent fracture-induced anisotropic media, derived from the results of Bakulin *et al.* (1999a, 1999b).

For all models, I compute all three exact reflection coefficients (i.e. R_{PP}, R_{PSV} and R_{PSH}), their approximations and the corresponding absolute errors as functions of the incidence angle and azimuth, see Figures 2-10. The azimuth is measured from the x-axis of the reference coordinate system as introduced in Figure 1; the orientation of the x-axis is defined separately for each particular model. The approximate coefficient R_{PP}, shown for comparison, is determined using the equations of Vavryčuk and Pšenčík (1998). The exact R_{PSV} and R_{PSH} components are obtained by performing the projection of the exact R_{PS_1} and R_{PS_2} coefficients described above. Thus, an error associated with such a projection influences the final results. This may simulate the processing applied to real data prior to the PS-wave AVO analysis. Approximate R_{PSV} and R_{PSH} components are computed by using equations (39), (C1), (C2) and Table 1. The absolute error is determined as the absolute value of the difference between the exact and approximate coefficients.

Figures 2-4 show the R_{PP}, R_{PSV} and R_{PSH} coefficients (respectively) computed for an VTI/HTI interface. The VTI incidence halfspace represents a typical shale layer overlying an isotropic medium with vertical cracks resulting in HTI symmetry. In this model, the cracks are gas-filled and a moderate crack density of 5% is assumed. The medium parameters for both halfspaces can be found in the caption of Figure 2 (for more detail, see Bakulin *et al.*, 1999a). The x-axis of the reference coordinate system is horizontal and coincides with the symmetry axis of the HTI medium (perpendicular to the cracks).

The P-wave reflection coefficient in Figure 2 is well represented by the approximate equations. The shape of the approximate coefficient (i.e. its variation with the incidence and azimuthal angles) is basically identical to that of the exact coefficient. The relative error does not exceed 5% up to the incidence angle of 20°; for larger azimuths the accuracy remains high for larger incidence angles (the coefficient is relatively weak which results in higher relative errors in general). In the case of the R_{PSV} component (Figure 3), the absolute error is small for the whole angle region presented. The R_{PSV} component increases with the incidence angle from zero at normal incidence. Therefore, any estimates of the coefficient at small incidence angles will contain large relative errors. Very likely, such a small-incidence-angle reflection event will be strongly distorted by noise. Otherwise, the R_{PSV} component is approximated very well in this model. Finally, Figure 4 shows the R_{PSH} component. The shape of this component is also approximated quite well. However, the absolute errors are comparable with the coefficient itself. This should not be surprising since the component is very small (notice that the R_{PSH} component is globally zero for isotropic media) and thus

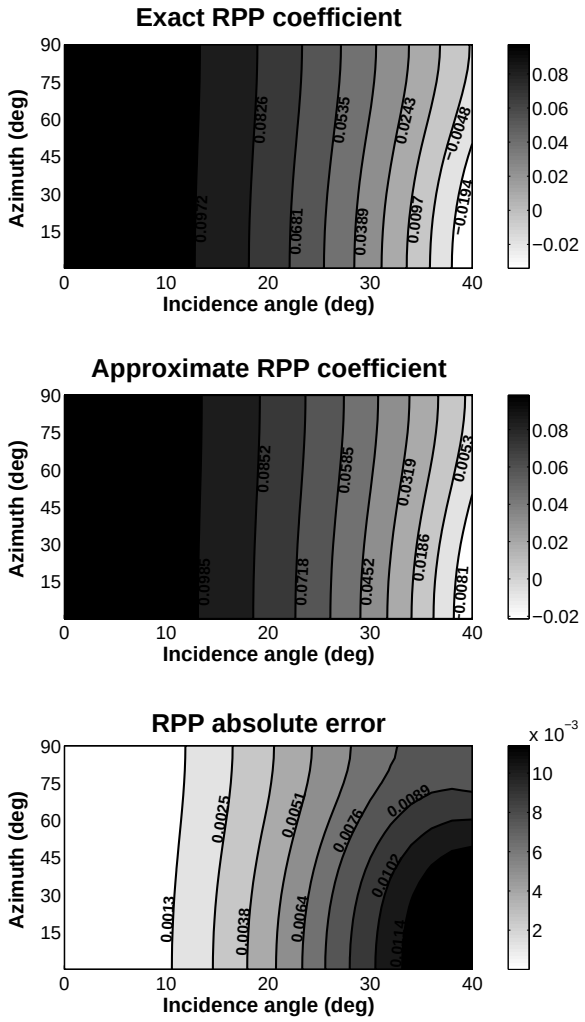

Figure 2. Reflection coefficient R_{PP} for a VTI/HTI interface as a function of the incidence angle and azimuth: the exact coefficient (top), the weak-contrast, weak-anisotropy approximation (middle) and the absolute error (bottom) defined as the difference between the exact and approximate coefficients. Medium parameters are as follows: VTI incidence halfspace: $\rho = 2.0\,\mathrm{g/cm^3}$, $V_{P0} = 2.9\,\mathrm{km/s}$, $V_{S0} = 1.5\,\mathrm{km/s}$, $\epsilon = 0.2$, $\delta = 0.1$, $\gamma = 0.1$; HTI reflecting halfspace: $\rho = 2.2\,\mathrm{g/cm^3}$, $V_{P0} = 3.3\,\mathrm{km/s}$, $V_{44} = 1.8\,\mathrm{km/s}$, $\epsilon^{(V)} = -0.13$, $\delta^{(V)} = -0.14$ and $\gamma^{(V)} = -0.053$; $V_{44} = \sqrt{A_{44}}$.

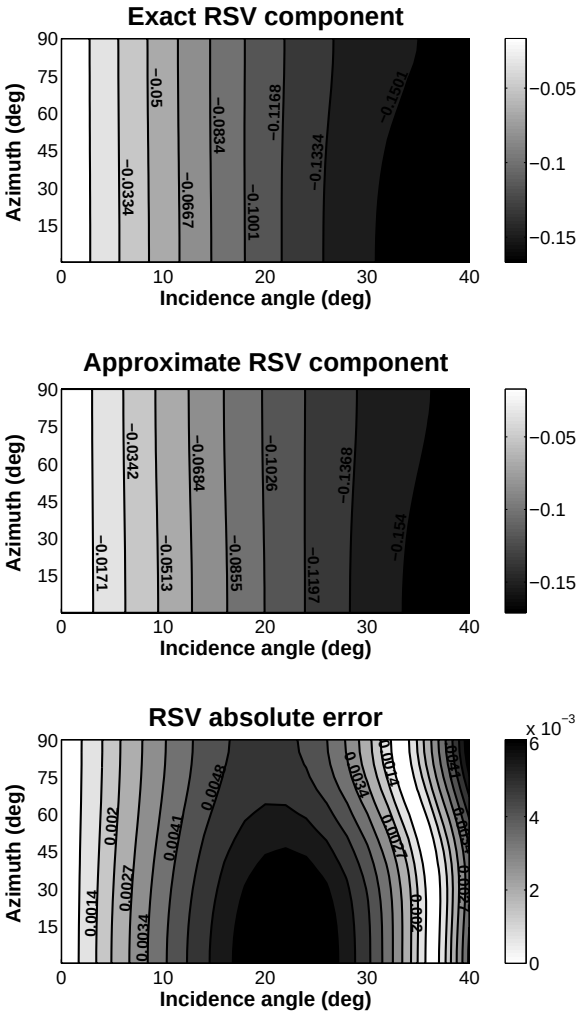

Figure 3. Component R_{PSV} of the PS-wave reflection coefficient for the VTI/HTI interface as in Figure 2 plotted as a function of the incidence angle and azimuth: the exact component (top), the weak-contrast, weak-anisotropy approximation (middle) and the absolute error (bottom) defined as the difference between the exact and approximate components.

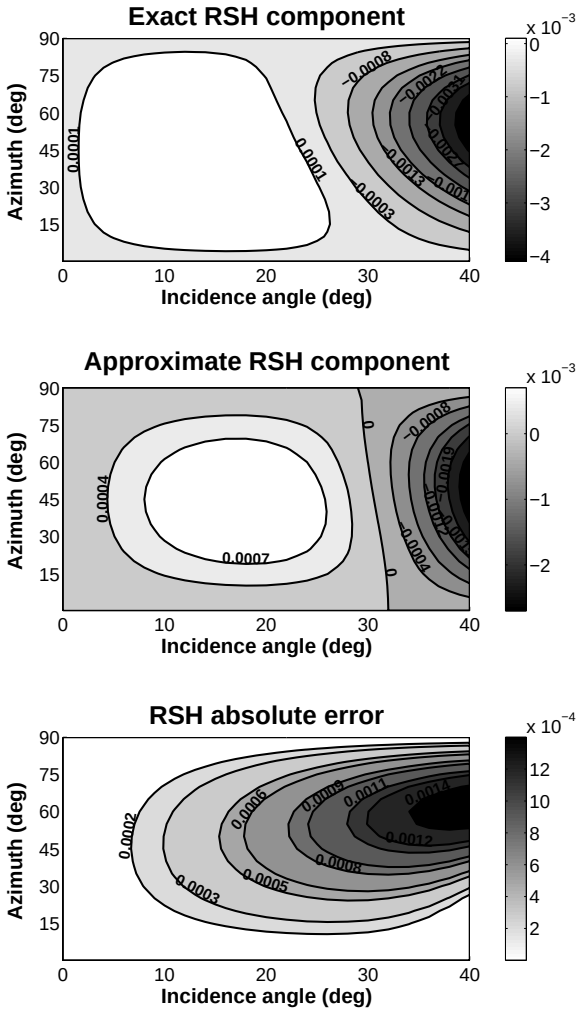

Figure 4. Component R_{PSH} of the PS-wave reflection coefficient for the VTI/HTI interface as in Figure 2 plotted as a function of the incidence angle and azimuth: the exact component (top), the weak-contrast, weak-anisotropy approximation (middle) and the absolute error (bottom) defined as the difference between the exact and approximate components.

large relative errors can be expected. Therefore, if R_{PSH} detected on real data, equations (39) and (C2) should be used for qualitative analysis rather than for quantitative estimates.

Figures 5-7 correspond to an interface between two orthorhombic media with mutually rotated vertical symmetry planes. Such a model can represent, for example, two mutually rotated vertical crack sets above each other embedded in an isotropic host rock. Each of the sets consists of two perpendicular crack systems with different crack densities. In the incidence halfspace, the crack density of the cracks parallel to the $[x_2, x_3]$ plane of the local coordinate system (one of the symmetry planes) is $e_1 = 3\%$, the perpendicular crack set (parallel to the other symmetry plane) has the crack density $e_2 = 5\%$ (for more details, see Bakulin *et al.*, 1999b). The cracks are dry and are embedded in the isotropic rock with P- and S-wave velocities 3.6 km/s and 2.3 km/s, respectively. In the reflecting halfspace, the crack sets are interchanged ($e_1 = 5\%$, $e_2 = 3\%$) and the isotropic host rock is characterized by the P- and S-wave velocities 4.17 km/s and 2.52 km/s, respectively. Additionally, the whole crack set of the reflecting halfspace is rotated with respect to the crack set of the incidence halfspace by the angle $\kappa = 30^\circ$. The resulting medium parameters of both halfspaces are provided in the caption of Figure 5. The reference coordinate system is associated to the incidence orthorhombic medium with the horizontal x-axis perpen-

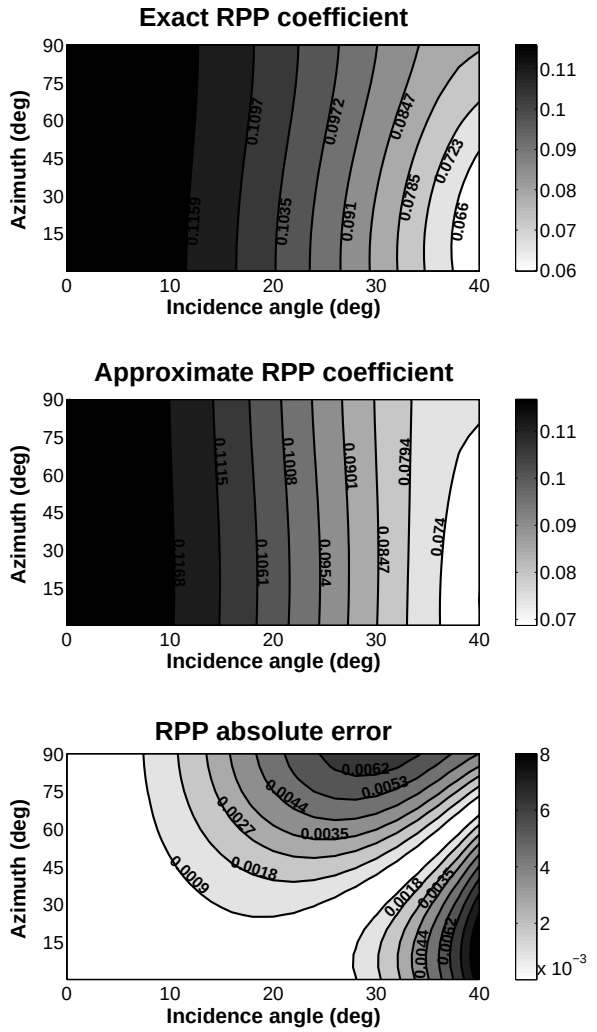

Figure 5. Reflection coefficient R_{PP} for an orthorhombic/orthorhombic interface as a function of the incidence angle and azimuth: the exact coefficient (top), the weak-contrast, weak-anisotropy approximation (middle) and the absolute error (bottom) defined as the difference between the exact and approximate coefficients. The vertical symmetry planes of the orthorhombic halfspaces are mutually rotated by the angle $\kappa = 30°$. Medium parameters are as follows: incidence medium: $\rho = 2.1$ g/cm^3 $V_{33} = 3.57$ km/s, $V_{44} = 2.16$ km/s, $\epsilon^{(1)} = -0.14$, $\delta^{(1)} = -0.14$, $\gamma^{(1)} = -0.06$, $\epsilon^{(2)} = -0.08$, $\delta^{(2)} = -0.08$, $\gamma^{(2)} = -0.04$, $\delta^{(3)} = -0.06$; reflecting medium: $\rho = 2.3$ g/cm^3, $V_{33} = 4.17$ km/s, $V_{44} = 2.52$ km/s, $\epsilon^{(1)} = -0.08$, $\delta^{(1)} = -0.08$, $\gamma^{(1)} = -0.04$, $\epsilon^{(2)} = -0.14$, $\delta^{(2)} = -0.14$, $\gamma^{(2)} = -0.06$, $\delta^{(3)} = 0.05$; $V_{33} = \sqrt{A_{33}}$ and $V_{44} = \sqrt{A_{44}}$.

dicular to the $[x_2, x_3]$ symmetry plane. This model represents the most general configuration that can be treated by equations (39), (C1) and (C2).

Figure 5 shows a good accuracy of the approximation for the R_{PP} reflection coefficient. The absolute error generally increases for higher azimuths but is small for

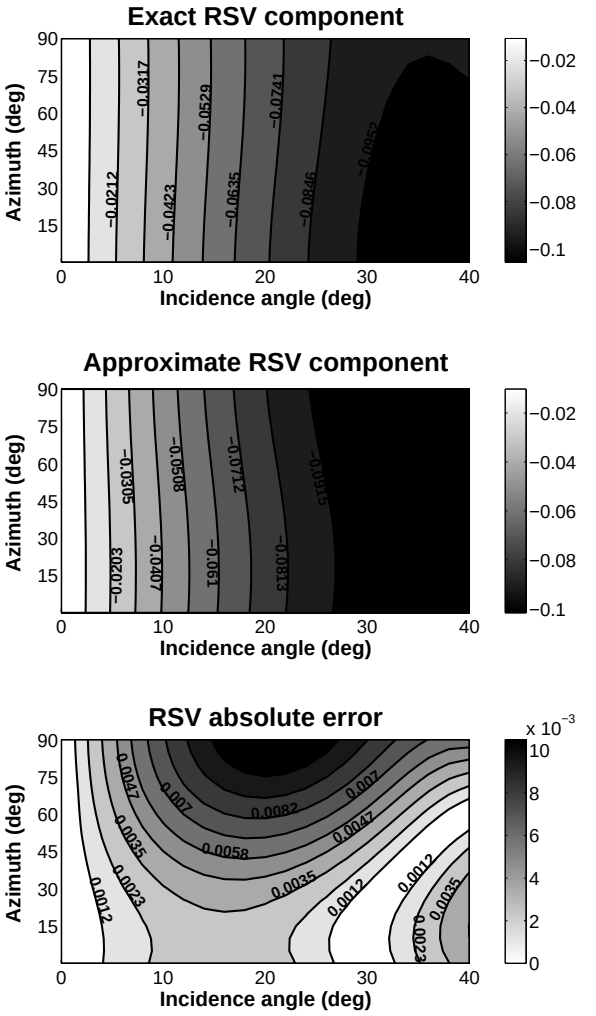

Figure 6. Component R_{PSV} of the PS-wave reflection coefficient for the orthorhombic/orthorhombic interface as in Figure 5 plotted as a function of the incidence angle and azimuth: the exact component (top), the weak-contrast, weak-anisotropy approximation (middle) and the absolute error (bottom) defined as the difference between the exact and approximate components.

incidence angles under 30°. Similar angle dependence of the error can be also observed for the R_{PSV} component (Figure 6). Here, the error is somewhat higher that that for R_{PP}. For small and moderate azimuths (up to 50°), however, the approximation works well. Also, the shape of the R_{PSH} approximation in Figure 7 is sufficiently accurate, especially for incidence angles up to 30°. Notice that the R_{PSH} component does not vanish for azimuths 0° and 90° as in the previous examples. This is due to the misalignment of the vertical symmetry planes of the incidence and reflecting halfspaces. Figures 5-7 suggest that expressions (39), (C1) and (C2) can work reasonably well even for complicated models.

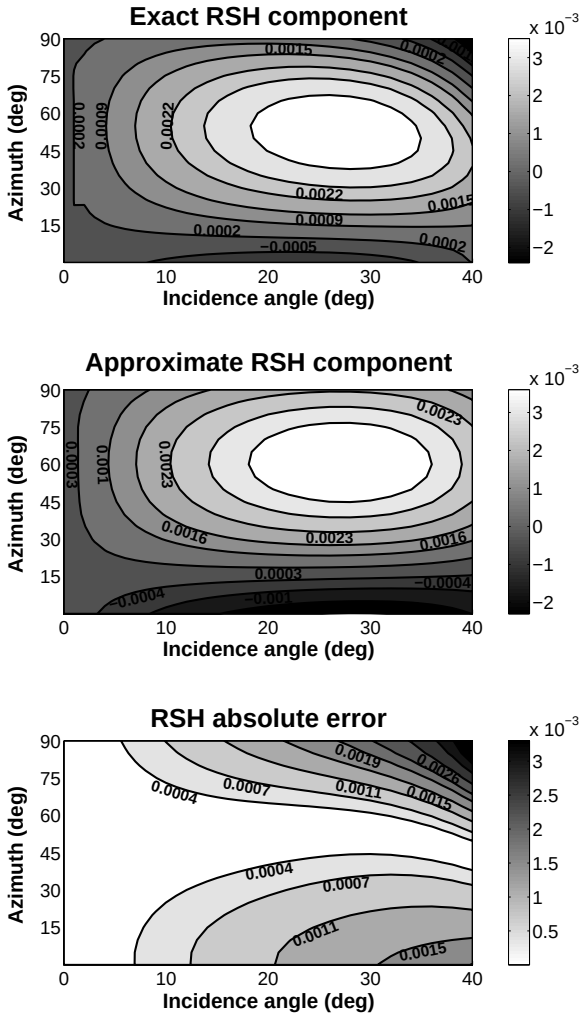

Figure 7. Component R_{PSH} of the PS-wave reflection coefficient for the orthorhombic/orthorhombic interface as in Figure 5 plotted as a function of the incidence angle and azimuth: the exact component (top), the weak-contrast, weak-anisotropy approximation (middle) and the absolute error (bottom) defined as the difference between the exact and approximate components.

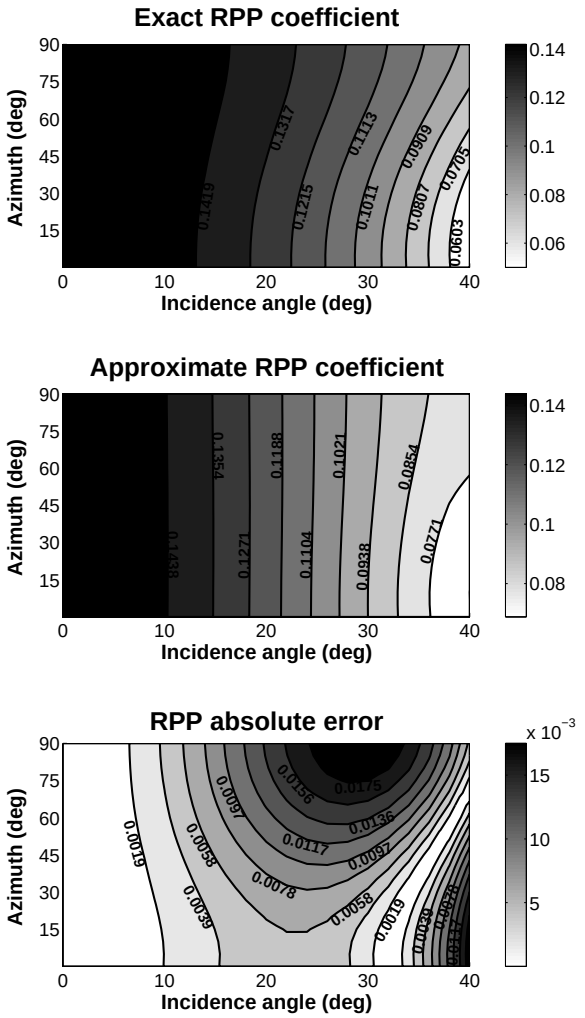

Figure 8. Reflection coefficient R_{PP} for a strong-contrast, strong-anisotropy orthorhombic/orthorhombic interface as a function of the incidence angle and azimuth: the exact coefficient (top), the weak-contrast, weak-anisotropy approximation (middle) and the absolute error (bottom) defined as the difference between the exact and approximate coefficients. The vertical symmetry planes of the orthorhombic halfspaces are mutually rotated by the angle $\kappa = 30^\circ$. Medium parameters are as follows: incidence medium: $\rho = 2.0$ g/cm^3 $V_{33} = 3.4$ km/s, $V_{44} = 1.8$ km/s, $\epsilon^{(1)} = -0.27$, $\delta^{(1)} = -0.28$, $\gamma^{(1)} = -0.1$, $\epsilon^{(2)} = -0.19$, $\delta^{(2)} = -0.20$, $\gamma^{(2)} = -0.07$, $\delta^{(3)} = -0.11$; reflecting medium: $\rho = 2.2$ g/cm^3, $V_{33} = 4.2$ km/s, $V_{44} = 2.4$ km/s, $\epsilon^{(1)} = -0.18$, $\delta^{(1)} = -0.20$, $\gamma^{(1)} = -0.08$, $\epsilon^{(2)} = -0.24$, $\delta^{(2)} = -0.25$, $\gamma^{(2)} = -0.1$, $\delta^{(3)} = 0.06$; $V_{33} = \sqrt{A_{33}}$ and $V_{44} = \sqrt{A_{44}}$.

The last model (Figures 8-10) is derived from the previous one by increasing the anisotropy in both halfspaces (by increasing crack densities to more than 10% here). Thus, the anisotropy becomes strong and the approximations are expected to fail.

Surprisingly, in the case of R_{PP} (Figure 8), the approximations work even better than for the previous model. I attribute this improvement to the general increase in the R_{PP} coefficient compared to the previous model, which eventually yields a more stable result. On the other hand, the accuracy of the R_{PSV} component decreased, as expected (Figure 9). Also, the azimuthal variation of R_{PSV} is not approximated sufficiently. A similar failure can be observed for the R_{PSH} component (Figure 10). Note that the exact R_{PSV} and R_{PSH} components have been obtained by the projection described above [equation (44)] that becomes inaccurate for strongly anisotropic incidence medium.

Extensive numerical tests indicate that the accu-

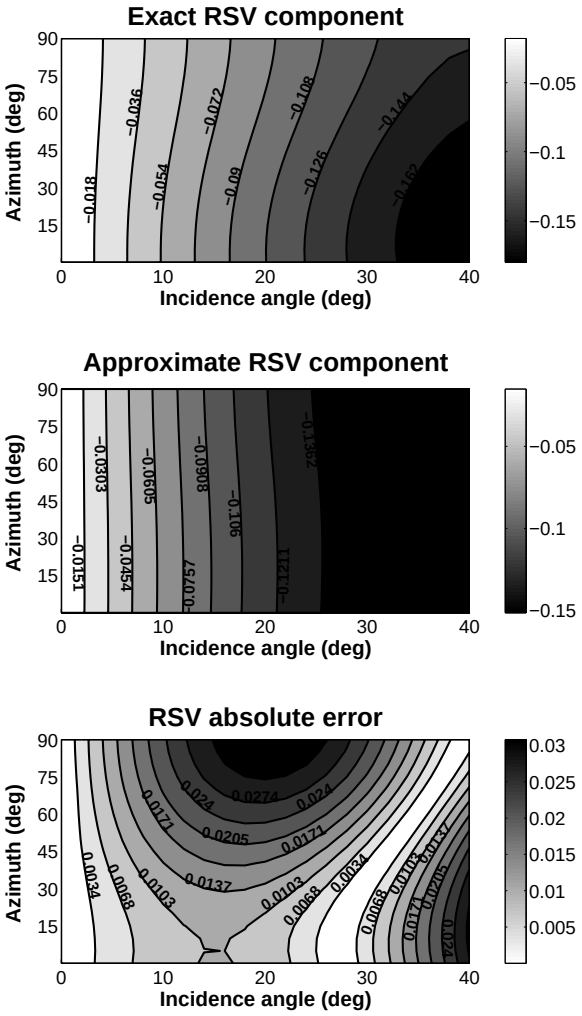

Figure 9. Component R_{PSV} of the PS-wave reflection coefficient for the strong-contrast, strong-anisotropy orthorhombic/orthorhombic interface as in Figure 8 plotted as a function of the incidence angle and azimuth: the exact component (top), the weak-contrast, weak-anisotropy approximation (middle) and the absolute error (bottom) defined as the difference between the exact and approximate components.

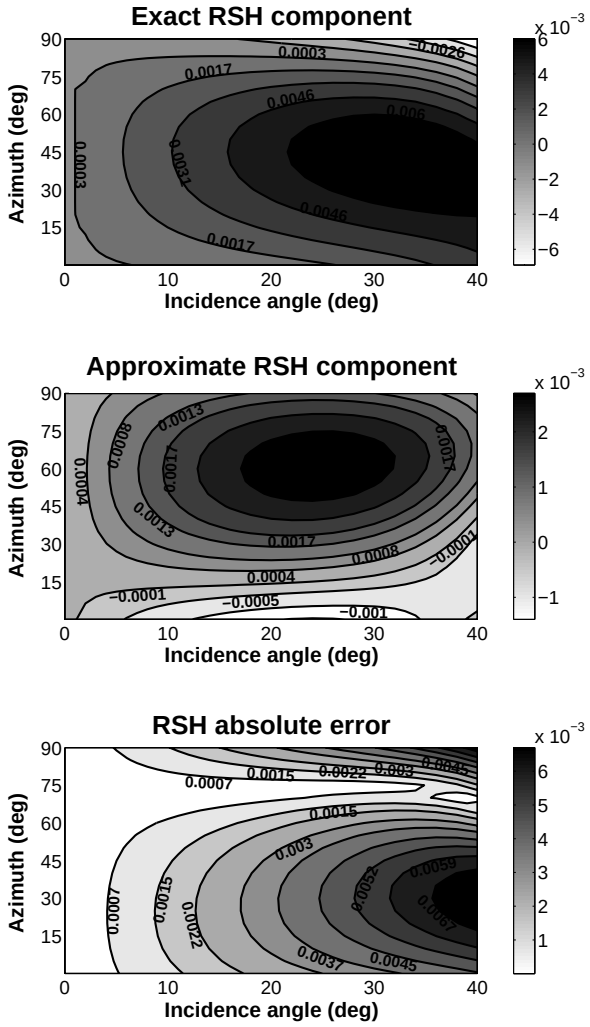

Figure 10. Component R_{PSH} of the PS-wave reflection coefficient for the strong-contrast, strong-anisotropy orthorhombic/orthorhombic interface as in Figure 8 plotted as a function of the incidence angle and azimuth: the exact component (top), the weak-contrast, weak-anisotropy approximation (middle) and the absolute error (bottom) defined as the difference between the exact and approximate components.

racy of the R_{PSV} and R_{PSH} approximations generally decreases for lower anisotropic symmetries, such as orthorhombic media. However, the approximations may work still sufficiently well, even for relatively strong contrasts and strong anisotropy.

Summary

Here, I presented first-order approximations for converted-wave reflection coefficients R_{PS_1} and R_{PS_2} at a weak horizontal interface separating two weakly anisotropic media of arbitrary symmetry. I used the approach described by Vavryčuk and Pšenčík (1998) for PP reflection/transmission coefficients. The general expressions were specified for an orthorhombic/orthorhombic interface with mutually rotated vertical symmetry planes using Thomsen-type medium parameterization. Also, simple forms of the reflection coefficient approximations for small incidence angles (i.e. PS-wave AVO gradients) were obtained. The final expressions can be immediately applied for any combination of isotropic, VTI, HTI and orthorhombic halfspaces.

As expected, the expressions for the coefficients R_{PS_1} and R_{PS_2} are more complicated than the corresponding expressions for R_{PP}. The coefficients R_{PS_1} and

R_{PS_2} also contain a nonlinear polarization angle Φ characterizing the orientation of the S-wave polarization vectors in the anisotropic incidence halfspace. To extract the linear parts of the coefficients (denoted as R_{PSV} and R_{PSH} here), not only the reflection coefficients but also the polarization directions of both S-waves must be known. Moreover, R_{PS_1} and R_{PS_2} coefficients should not be used at S-wave singular points. Clearly, the analysis of PS-wave reflection coefficients is more involved than that of PP-wave reflection coefficients.

Numerical tests show good overall agreement of the derived approximations with the corresponding exact coefficients for most models. The accuracy of the R_{PSV} component is usually comparable to that of the R_{PP} approximations. However, whereas the R_{PP} approximations are mostly applicable for small and moderate incidence angles, the R_{PSV} approximations frequently work even for relatively large incidence angles. On the other hand, small-incidence-angle PS reflections are weak in general and thus likely distorted by noise.

The R_{PSH} component is a direct indicator of anisotropy (R_{SH} is zero for isotropic models). Its azimuthal variation is more significant than that of R_{PP} or R_{SV}. This fact can be used to obtain additional information about the medium (e.g. the directions of symmetry planes), if the component can be estimated from the data. Unfortunately, R_{PSH} is usually small and is likely to be distorted by noise. However, it may still be possible to find local extrema of the R_{PSH} component as a function of azimuth and use them to constrain the model.

Azimuthal variation of both R_{PSV} and R_{PSH} components is well-reproduced by the approximations for most models used here. However, decreasing accuracy can be generally expected for lower anisotropic symmetries, such as orthorhombic models. On the other hand, numerical tests also reveal that both R_{PSV} and R_{PSH} approximations may still work quite well even for some strongly anisotropic models. The results indicate a trade-off between the weak-contrast, weak-anisotropy condition and the stability of the approximations.

R_{PS_1} and R_{PS_2} coefficients can be analyzed for arbitrarily anisotropic halfspaces as well. The next logical step is to specify the general equations for TI halfspaces with arbitrarily tilted symmetry axes, and for orthorhombic halfspaces with no horizontal symmetry planes. However, the final expressions would be more complicated due to the presence of additional angles (two more angles for TI media or three more angles for orthorhombic media for each halfspace). This problem could be partially eliminated if a different parameterization of anisotropic media was adopted, such as the one introduced by Pšenčík and Gajewski (1998). Resulting expressions for R_{PS_1} and R_{PS_2} coefficients could be used not only for a horizontal interface, but also for an interface with an arbitrary dip.

Together with the R_{PP} coefficient, R_{PS_1} and R_{PS_2} coefficients may provide a powerful tool for more stable and reliable AVO inversion. Such an inversion, however, will require a high quality 3-D 3-C data.

Acknowledgments

I thank Ilya Tsvankin and Vladimir Grechka for their valuable advice during this research and for their suggestions in improving the manuscript. I am also grateful to members of the A(nisotropy)-team of the Center for Wave Phenomena at the Colorado School of Mines for many helpful comments. My special thanks to Ivan Pšenčík (Geophysical Institute, Academy of Sciences, Czech Republic) for numerous stimulating discussions.

References

Aki, K.,& Richards, P.G.1980. *Quantitative Seismology: theory and methods.* Vol.1. W. N. Freeman & Co., San Francisco.

Alvarez, K., Donati, M., Aldana, M. 1999. AVO analysis for converted waves. *Pages 876-879 of: 69th Annual Internat. Mtg., Soc. Expl. Geophys., Expanded Abstracts.*

Bakulin, A., Grechka, V., and Tsvankin, I. 1999a. Estimation of fracture parameters from reflection seismic data, Part I: HTI model due to a single fracture set. *Pages 18-34 of: CWP Project Review*, CWP, Colorado School of Mines.

Bakulin, A., Grechka, V., and Tsvankin, I. 1999b. Estimation of fracture parameters from reflection seismic data, Part II: fractured models with orthorhombic symmetry. *Pages 35-52 of: CWP Project Review*, CWP, Colorado School of Mines.

Banik, N.C. 1987. An effective anisotropy parameter in transversely isotropic media. *Geophysics,* **52**(12), 1654-1664.

Bortfeld, R. 1961. Approximation to the reflection coefficients of plane longitudinal and transverse waves. *Geophysical Prospecting*, **9**, 485-502.

Červený, V., Molotkov, I. A., and Pšenčík, I. 1977. *Ray method in seismology.* Universita Karlova, Praha.

Daley, P. F., & Hron, F. 1977. Reflection and transmission coefficients for transversely isotropic solids. *Bull. Seis. Soc. Am.*, **67**, 661-675.

Donati, S. M. 1998. Making AVO analysis for converted waves a practical issue. *Pages 2060-2063 of: 68th Annual Internat. Mtg., Soc. Expl. Geophys., Expanded Abstracts.*

Graebner, M. 1992. Plane-wave reflection and transmission coefficients for a transversely isotropic solid (short note). *Geophysics*, **57** (11), 1512-1519.

Grechka, V., and Tsvankin, I., 1998. 3-D description of normal moveout for anisotropic media: *Geophysics*, **63**, 1079-1092.

Jech, J., and Pšenčík, I. 1989. First-order perturbation method for anisotropic media. *Geophys. J. Int.*, **99**, 369-376.

Jin, S. 1999. Characterizing reservoir by using jointly P- and S-wave AVO analyses. *Pages 687-690 of: 69th Annual Internat. Mtg., Soc. Expl. Geophys., Expanded Abstracts.*

Keith, C. M., & Crampin, S. 1977. Seismic body waves in anisotropic media: reflection and refraction at a plane interface. *Geophys. J. R. astr. Soc.*, **49**, 181-208.

Larsen, A. J., Margrave, F. G., and Lu, H-X. 1999. AVO analysis by simultaneous P-P and P-S weighted stacking applied to 3C-3D seismic data. *Pages 721-724 of: 69th Annual Internat. Mtg., Soc. Expl. Geophys., Expanded Abstracts.*

Li, X-Y., Kühnel, T., and MacBeth, C. 1996. Mixed mode AVO response in fractured media. *Pages 1822-1825 of: 66th Annual Internat. Mtg., Soc. Expl. Geophys., Expanded Abstracts.*

Miley, P. M. 1999. Overpressure prediction using converted mode reflections from base salt. *Pages 880-883 of: 69th Annual Internat. Mtg., Soc. Expl. Geophys., Expanded Abstracts.*

Musgrave, M. J. P. 1970. *Crystal acoustics.* Holden Day, San Francisco.

Nefedkina, T., and Buzlukov, V. 1999. Seismic dynamic inversion using multiwave AVO data. *Pages 888-891 of: 69th Annual Internat. Mtg., Soc. Expl. Geophys., Expanded Abstracts.*

Pšenčík, I. 1998. Green's functions for inhomogeneous weakly anisotropic media. *Geophys. J. Int.*, **135**, 279-288.

Pšenčík, I., and Gajewski, D. 1998. Polarization, phase velocity and NMO velocity of qP waves in arbitrary weakly anisotropic media. *Geophysics*, **63**, 1754-1766.

Pšenčík, I., and Vavryčuk, V. 1998. Weak contrast PP wave displacement R/T coefficients in weakly anisotropic elastic media. *Pure Appl. Geophys.*, **151**, 699-718.

Pšenčík, I., Martins, J. L. 1999. Properties of approximate weak contrast PP reflection/transmission coefficients for weakly anisotropic media. *Submitted to Geophysics.*

Richards, P. G., & Frasier, C. W. 1976. Scattering of elastic waves from depth-dependent inhomogeneities. *Geophysics*, **41** (3), 441-458.

Rüger, A. 1996. *Reflection coefficients and azimuthal AVO analysis in anisotropic media.* Ph.D. Thesis, Center for Wave Phenomena, Golden, Colorado.

Rüger, A. 1997. P-wave reflection coefficients for transversely isotropic models with vertical and horizontal axis of symmetry: Geophysics, **62**, 713-722.

Rüger, A. 1998. Variation of P-wave reflectivity with offset and azimuth in anisotropic media: Geophysics, **63** (3), 935-947.

Sayers, C. M. 1994. P-wave propagation in weakly anisotropic media. *Geophys. J. Int.*, **116**, 799-805.

Shuey, R. T. 1985. A simplification of Zoeppritz-equations. *Geophysics*, **50** (4), 609-614.

Thomsen, L. 1986. Weak elastic anisotropy. *Geophysics*, **51** (10), 1954-1966.

Thomsen, L. 1993. Weak anisotropic reflections. *In: Offset dependent reflectivity (Castagna and Backus, Eds.), SEG, Tulsa.*

Tsvankin, I. 1996. P-wave signatures and notation for transversely isotropic media: an overview. *Geophysics*, **61** (2), 467-483.

Tsvankin, I. 1997a. Reflection moveout and parameter estimation for horizontal transverse isotropy. *Geophysics*, **62** (2), 614-629.

Tsvankin, I. 1997b. Anisotropic parameters and P-wave velocity in orthorhombic media. *Geophysics*, **62** (4), 1292-1309.

Vavryčuk, V. 1999. Weak-contrast reflection/transmission coefficients in weakly anisotropic elastic media: P-wave incidence. *Geophys. J. Int.*, **138**, 553-562.

Vavryčuk, V., and Pšenčík, I. 1998. PP-wave reflection coefficients in weakly anisotropic elastic media. *Geophysics*, **63** (6), 2129-2141.

Zoeppritz, K. 1919. Erdbebenwellen, on the reflection and penetration of seismic waves through unstable layers. *Göttinger Nachrichten*, **1** (VII B), 66-84.

APPENDIX A: Background polarization-traction matrix $\hat{\mathbf{C}}^0$ and weak anisotropy perturbations of polarization and normalized traction vectors $\delta\boldsymbol{g}$ and $\delta\boldsymbol{X}$

To evaluate the approximations of reflection/transmission coefficients (14), the background polarization-traction matrix $\hat{\mathbf{C}}^0$ must be derived. From relations (3), (6), (15), (16), (17) and (18) one can obtain the following form of the matrix $\hat{\mathbf{C}}^0$:

$$\hat{\mathbf{C}}^0 = \begin{pmatrix} -\beta p_3^{0S}\cos\Phi & \beta p_3^{0S}\sin\Phi & \alpha p_1^0 & -\beta p_3^{0S}\cos\Psi & \beta p_3^{0S}\sin\Psi & -\alpha p_1^0 \\ \sin\Phi & \cos\Phi & 0 & -\sin\Psi & -\cos\Psi & 0 \\ -\beta p_1^0\cos\Phi & \beta p_1^0\sin\Phi & -\alpha p_3^{0P} & \beta p_1^0\cos\Psi & -\beta p_1^0\sin\Psi & -\alpha p_3^{0P} \\ \beta Y\cos\Phi & -\beta Y\sin\Phi & -Z_P & -\beta Y\cos\Psi & \beta Y\sin\Psi & -Z_P \\ -\rho^0\beta^2 p_3^{0S}\sin\Phi & -\rho^0\beta^2 p_3^{0S}\cos\Phi & 0 & -\rho^0\beta^2 p_3^{0S}\sin\Psi & -\rho^0\beta^2 p_3^{0S}\cos\Psi & 0 \\ Z_S\cos\Phi & -Z_S\sin\Phi & \alpha Y & Z_S\cos\Psi & -Z_S\sin\Psi & -\alpha Y \end{pmatrix}, \tag{A1}$$

where Z_P, Z_S and Y are defined as

$$\begin{aligned} Z_P &= 2\alpha\rho^0\beta^2 p_1^0 p_3^{0P}, \\ Z_S &= 2\rho^0\beta^3 p_1^0 p_3^{0S}, \\ Y &= \rho^0(1-2\beta^2(p_1^0)^2). \end{aligned}$$

The inverse of the matrix $\hat{\mathbf{C}}^0$ has been derived in Vavryčuk and Pšenčík (1998):

$$(\hat{\mathbf{C}}^0)^{-1} = \begin{pmatrix} -\frac{\beta^2 p_1^0 Y\cos\Phi}{Z_S} & \frac{\sin\Phi}{2} & -\beta p_1^0\cos\Phi & \frac{\cos\Phi}{2\rho^0\beta} & -\frac{\beta p_1^0\sin\Phi}{Z_S} & \frac{\beta^2(p_1^0)^2\cos\Phi}{Z_S} \\ \frac{\beta^2 p_1^0 Y\sin\Phi}{Z_S} & \frac{\cos\Phi}{2} & \beta p_1^0\sin\Phi & -\frac{\sin\Phi}{2\rho^0\beta} & -\frac{\beta p_1^0\cos\Phi}{Z_S} & -\frac{\beta^2(p_1^0)^2\sin\Phi}{Z_S} \\ \frac{\beta^2 p_1^0}{\alpha} & 0 & -\frac{\beta^2 p_1^0 Y}{Z_P} & -\frac{\beta^2(p_1^0)^2}{Z_P} & 0 & \frac{1}{2\rho^0\alpha} \\ -\frac{\beta^2 p_1^0 Y\cos\Psi}{Z_S} & -\frac{\sin\Psi}{2} & \beta p_1^0\cos\Psi & -\frac{\cos\Psi}{2\rho^0\beta} & -\frac{\beta p_1^0\sin\Psi}{Z_S} & \frac{\beta^2(p_1^0)^2\cos\Psi}{Z_S} \\ \frac{\beta^2 p_1^0 Y\sin\Psi}{Z_S} & -\frac{\cos\Psi}{2} & -\beta p_1^0\sin\Psi & \frac{\sin\Psi}{2\rho^0\beta} & -\frac{\beta p_1^0\cos\Psi}{Z_S} & -\frac{\beta^2(p_1^0)^2\sin\Psi}{Z_S} \\ -\frac{\beta^2 p_1^0}{\alpha} & 0 & -\frac{\beta^2 p_1^0 Y}{Z_P} & -\frac{\beta^2(p_1^0)^2}{Z_P} & 0 & -\frac{1}{2\rho^0\alpha} \end{pmatrix}. \tag{A2}$$

The expression (A2) is substituted into equation (20) that contains first-order perturbations of the polarization and normalized traction vectors $\delta\boldsymbol{g}^{(0)}$, $\delta\boldsymbol{g}^{(6)}$ and $\delta\boldsymbol{X}^{(0)}$, $\delta\boldsymbol{X}^{(6)}$, respectively. The derivation of the perturbations has been described in detail by Jech and Pšenčík (1989). Based on their derivations, it can be shown that (see also Vavryčuk and Pšenčík, 1998)

$$\delta g_i^{(6)} - \delta g_i^{(0)} = (\delta c^{(6)} - \delta c^{(0)})\left[p_i^{0(0)} - \frac{n_i}{\alpha^2(n_k p_k^{0(0)})}\right] + (\delta G_i^{(6)} - \delta G_i^{(0)}), \tag{A3}$$

where i represents the i-th vector component. Here, $p_i^{0(0)}$ is the slowness vector of the incidence P-wave in the background medium [equation (15)], n_i is the normal to the interface and α is the P-wave background velocity. $\delta c^{(N)}$ is the deviation of the phase velocity (its magnitude) of the incidence (N=0) or transmitted (N=6) P-wave in the weakly anisotropic medium from the corresponding phase velocity in the isotropic background. By a linear perturbation of the Christoffel equation, Jech and Pšenčík (1989) obtained

$$\begin{aligned} \delta c^{(0)} &= \frac{1}{2}\alpha\delta a_{ijkl}^{(1)} p_i^{0(0)} g_j^{0(0)} g_k^{0(0)} p_l^{0(0)}, \\ \delta c^{(6)} &= \frac{1}{2}\alpha\delta a_{ijkl}^{(2)} p_i^{0(0)} g_j^{0(0)} g_k^{0(0)} p_l^{0(0)}, \end{aligned} \tag{A4}$$

where $g_i^{0(0)}$ is given in relations (16) and $a_{ijkl}^{(I)}$ by relation (10). It immediately follows that

$$\delta c^{(6)} - \delta c^{(0)} = \frac{1}{2}\alpha\Delta a_{ijkl} p_i^{0(0)} g_j^{0(0)} g_k^{0(0)} p_l^{0(0)}, \tag{A5}$$

where

$$\Delta a_{ijkl} = \delta a_{ijkl}^{(2)} - \delta a_{ijkl}^{(1)} = a_{ijkl}^{(2)} - a_{ijkl}^{(1)} \tag{A6}$$

are the contrasts of the elastic parameters across the interface.

Finally, the vectors $\delta G_i^{(N)}$ in (A3) describe the deviations of the polarization vectors in the weakly anisotropic medium from the corresponding polarization vectors in the isotropic background caused *purely* by the anisotropy.

Their expressions are given in Jech and Pšenčík (1989). In a similar fashion as in the previous paragraph, it is possible to write

$$\delta G_m^{(6)} - \delta G_m^{(0)} = \frac{\alpha}{\alpha^2 - \beta^2} \Delta a_{ijkl} p_i^{0(0)} g_j^{0(0)} g_k^{0(0)} (\delta_{lm} - g_l^{0(0)} g_m^{0(0)}), \tag{A7}$$

where δ_{lm} is Kronecker's delta.

Notice, that equation (A3) describes the perturbations of the polarization vectors from the background due to both the elastic parameter contrasts across the interface and the anisotropy.

From equations (3), taking into account that $\boldsymbol{n} = (0, 0, 1)$, the difference of the first-order perturbations of amplitude-normalized traction vectors can be obtained as

$$\begin{aligned} \delta X_i^{(6)} - \delta X_i^{(0)} = {} & \Delta\rho a_{i3kl}^0 g_k^{0(0)} p_l^{0(0)} + \rho^0 \Delta a_{i3kl} g_k^{0(0)} p_l^{0(0)} + \\ & \rho^0 a_{i3kl}^0 (\delta g_k^{(6)} - \delta g_k^{(0)}) p_l^{0(0)} + \rho^0 a_{i3kl}^0 g_k^{0(0)} (\delta p_l^{(6)} - \delta p_l^{(0)}), \end{aligned} \tag{A8}$$

The quantities a_{i3kl}^0 and ρ^0 are defined in equations (10), Δa_{i3kl} is given by (A6). Similarly, $\Delta\rho = \rho^{(2)} - \rho^{(1)}$ is the density contrast across the interface. The difference $\delta g_k^{(6)} - \delta g_k^{(0)}$ is specified by relation (A3). The term $\delta p_l^{(6)} - \delta p_l^{(0)}$ has an analogous physical meaning as $\delta g_l^{(6)} - \delta g_l^{(0)}$; however, it is now applied to the slowness vector. Using expressions in Jech and Pšenčík (1989) and Vavryčuk and Pšenčík (1998) yields the relation

$$\delta p_i^{(6)} - \delta p_i^{(0)} = -\frac{\delta c^{(6)} - \delta c^{(0)}}{\alpha^3 p_3^{0(0)}}, \tag{A9}$$

where all quantities are specified above. By substituting equations (A3) and (A5)-(A9) into equation (20), the approximate P-wave incidence reflection/transmission coefficients can be found.

APPENDIX B: General explicit expressions for the reflection coefficients R_{PS_1} and R_{PS_2}

To generalize the reflection coefficient R_{PS_1} (21) for an arbitrary azimuth ψ of the incidence plane [see the convention in Figure 1a], the medium parameters ΔA_{ij} must be expressed in terms of $\Delta A'_{ij}$ defined in the reference coordinate system. The tensor rotation is controlled by the following matrix of the directional cosines:

$$\hat{\mathbf{R}} = \begin{pmatrix} \cos\psi & -\sin\psi & 0 \\ \sin\psi & \cos\psi & 0 \\ 0 & 0 & 1 \end{pmatrix}. \tag{B1}$$

Applying matrix (B1) to the elements $\Delta A'_{ij}$ yields

$$\begin{aligned} \Delta A_{11} &= \Delta A'_{11}\cos^4\psi + 2\Delta A'_{12}\cos^2\psi\sin^2\psi + 4\Delta A'_{16}\cos^3\psi\sin\psi + \\ &\quad \Delta A'_{22}\sin^4\psi + 4\Delta A'_{26}\cos\psi\sin^3\psi + 4\Delta A'_{66}\cos^2\psi\sin^2\psi, \\ \Delta A_{13} &= \Delta A'_{13}\cos^2\psi + \Delta A'_{23}\sin^2\psi + 2\Delta A'_{36}\cos\psi\sin\psi, \\ \Delta A_{14} &= \Delta A'_{14}\cos^3 - \Delta A'_{15}\cos^2\psi\sin\psi + \Delta A'_{24}\cos\psi\sin^2\psi - \Delta A'_{25}\sin^3\psi + \\ &\quad 2\Delta A'_{46}\cos^2\psi\sin\psi - 2\Delta A'_{56}\cos\psi\sin^2\psi, \\ \Delta A_{15} &= \Delta A'_{14}\cos^2\psi\sin\psi + \Delta A'_{15}\cos^3\psi + \Delta A'_{24}\sin^3\psi + \Delta A'_{25}\cos\psi\sin^2\psi + \\ &\quad 2\Delta A'_{46}\cos\psi\sin^2\psi + 2\Delta A'_{56}\cos^2\psi\sin\psi, \\ \Delta A_{16} &= -\Delta A'_{11}\cos^3\psi\sin\psi + \Delta A'_{12}(\cos^3\psi\sin\psi - \cos\psi\sin^3\psi) + \\ &\quad \Delta A'_{16}(\cos^4\psi - 3\cos^2\psi\sin^2\psi) + \Delta A'_{26}(3\cos^2\psi\sin^2\psi - \sin^4\psi) + \\ &\quad \Delta A'_{66}(2\cos^3\psi\sin\psi - 2\cos\psi\sin^3\psi), \\ \Delta A_{33} &= \Delta A'_{33}, \\ \Delta A_{34} &= \Delta A'_{34}\cos\psi - \Delta A'_{35}\sin\psi, \\ \Delta A_{35} &= \Delta A'_{34}\sin\psi + \Delta A'_{35}\cos\psi, \\ \Delta A_{36} &= -\Delta A'_{13}\cos\psi\sin\psi + \Delta A'_{23}\cos\psi\sin\psi + \Delta A'_{36}(\cos^2\psi - \sin^2\psi), \\ \Delta A_{45} &= \Delta A'_{44}\cos\psi\sin\psi + \Delta A'_{45}(\cos^2\psi - \sin^2\psi) - \Delta A'_{55}\cos\psi\sin\psi, \\ \Delta A_{55} &= \Delta A'_{44}\sin^2\psi\sin\psi + 2\Delta A'_{45}\cos\psi\sin\psi + \Delta A'_{55}\cos^2\psi, \end{aligned} \tag{B2}$$

$$\Delta A_{56} = -\Delta A'_{14}\cos\psi\sin^2\psi - \Delta A'_{15}\cos^2\psi\sin\psi + \Delta A'_{24}\cos\psi\sin^2\psi + \Delta A'_{25}\cos^2\psi\sin\psi + \Delta A'_{46}(\cos^2\psi\sin\psi - \sin^3\psi) + \Delta A'_{56}(\cos^3\psi - \cos\psi\sin^2\psi).$$

Relations (B2) are used to derive the approximations (23) and (24) for the azimuthally dependent reflection coefficients R_{PS1} and R_{PS2} valid for arbitrarily anisotropic halfspaces. The coefficients contain R_{PSV} and R_{PSH} components given by

$$\begin{aligned} R_{PSV} &= v_1 + v_2\sin^2 i + v_3\sin^4 i + v_4\cos i\sin i + v_5\cos i\sin^3 i + \\ &\quad v_6\frac{\sin i}{\cos j} + v_7\frac{\sin^3 i}{\cos j} + v_8\frac{sin^5 i}{\cos j} + v_9\frac{\cos i}{\cos j} + v_{10}\frac{\cos i\sin^2 i}{\cos j} + v_{11}\frac{\cos i\sin^4 i}{\cos j}, \\ R_{PSH} &= h_1\sin i + h_2\sin^3 i + h_3\cos i + h_4\cos i\sin^2 i + \\ &\quad h_5\frac{1}{\cos j} + h_6\frac{\sin^2 i}{\cos j} + h_7\frac{\sin^4 i}{\cos j} + h_8\frac{\cos i\sin i}{\cos j} + h_9\frac{\cos i\sin^3 i}{\cos j}, \end{aligned} \tag{B3}$$

where the coefficients v_i and h_i are as follows:

$$\begin{aligned} v_1 &= \frac{\alpha}{2\beta(\alpha^2-\beta^2)}[\Delta A_{35}\cos\psi + \Delta A_{34}\sin\psi], \\ v_2 &= \frac{1}{2\alpha\beta(\alpha^2-\beta^2)}[-(\alpha^2+4\beta^2)(\Delta A_{35}\cos\psi + \Delta A_{34}\sin\psi) + \\ &\quad (\alpha^2+2\beta^2)(\Delta A_{15}\cos^3\psi + (\Delta A_{14}+2\Delta A_{56})\cos^2\psi\sin\psi + \\ &\quad (\Delta A_{25}+2\Delta A_{46})\cos\psi\sin^2\psi + \Delta A_{24}\sin^3\psi)], \\ v_3 &= \frac{2\beta}{\alpha(\alpha^2-\beta^2)}[-\Delta A_{15}\cos^3\psi - (\Delta A_{14}+2\Delta A_{56})\cos^2\psi\sin\psi + \\ &\quad (\Delta A_{34} - \Delta A_{24}\sin^2\psi)\sin\psi + (\Delta A_{35} - (\Delta A_{25}+2\Delta A_{46})\sin^2\psi)\cos\psi], \\ v_4 &= -\frac{\beta}{\alpha}\frac{\Delta\rho}{\rho^0} - \frac{1}{2\alpha\beta(\alpha^2-\beta^2)}[\beta^2(-\Delta A_{33} + \Delta A_{13}\cos^2\psi + \Delta A_{23}\sin^2\psi + \\ &\quad \Delta A_{36}\sin 2\psi) + 2\alpha^2(\Delta A_{55}\cos^2\psi + \Delta A_{44}\sin^2\psi + \Delta A_{45}\sin 2\psi)], \\ v_5 &= \frac{-1}{2\alpha(\alpha^2-\beta^2)}[\beta(\Delta A_{33} + \Delta A_{11}\cos^4\psi + 4\Delta A_{16}\cos^3\psi\sin\psi - \\ &\quad 2(\Delta A_{23}+2\Delta A_{44})\sin^2\psi + 4\Delta A_{26}\cos\psi\sin^3\psi + \Delta A_{22}\sin^4\psi - \\ &\quad 2(\Delta A_{13}+2\Delta A_{55} - (\Delta A_{12}+2\Delta A_{66})\sin^2\psi)\cos^2\psi - 2(\Delta A_{36} + \\ &\quad 2\Delta A_{45})\sin 2\psi)], \\ v_6 &= -\frac{1}{2}\frac{\Delta\rho}{\rho^0} + \frac{1}{2(\alpha^2-\beta^2)}[-\Delta A_{33} + (\Delta A_{13}+2\Delta A_{55})\cos^2\psi + \\ &\quad (\Delta A_{23}+2\Delta A_{44})\sin^2\psi + (\Delta A_{36}+2\Delta A_{45})\sin 2\psi], \\ v_7 &= \frac{\beta^2}{\alpha^2}\frac{\Delta\rho}{\rho^0} + \frac{1}{2\alpha^2(\alpha^2-\beta^2)}[\beta^2[\Delta A_{33} - (\Delta A_{13}+4\Delta A_{55})\cos^2\psi - \\ &\quad (\Delta A_{23}+4\Delta A_{44})\sin^2\psi - (\Delta A_{36}+4\Delta A_{45})\sin(2\psi)] + \alpha^2[\Delta A_{33} + \\ &\quad \Delta A_{11}\cos^4\psi + 4\Delta A_{16}\cos^3\psi\sin\psi - 2(\Delta A_{23}+\Delta A_{44})\sin^2\psi + \\ &\quad 4\Delta A_{26}\cos\psi\sin^3\psi + \Delta A_{22}\sin^4\psi - 2(\Delta A_{13}+\Delta A_{55} - \\ &\quad (\Delta A_{12}+2\Delta A_{66})\sin^2\psi)\cos^2\psi - 2(\Delta A_{36}+\Delta A_{45})\sin 2\psi]], \\ v_8 &= \frac{\beta^2}{2\alpha^2(\alpha^2-\beta^2)}[\Delta A_{33} + \Delta A_{11}\cos^4\psi + 4\Delta A_{16}\cos^3\psi\sin\psi - \\ &\quad 2(\Delta A_{23}+2\Delta A_{44})\sin^2\psi + 4\Delta A_{26}\cos\psi\sin^3\psi + \Delta A_{22}\sin^4\psi - \\ &\quad 2(\Delta A_{13}+2\Delta A_{55} - (\Delta A_{12}+2\Delta A_{66})\sin^2\psi)\cos^2\psi - \\ &\quad 2(\Delta A_{36}+2\Delta A_{45})\sin 2\psi], \\ v_9 &= \frac{1}{2(\beta^2-\alpha^2)}[\Delta A_{35}\cos\psi + \Delta A_{34}\sin\psi], \\ v_{10} &= \frac{1}{2\alpha^2(\alpha^2-\beta^2)}[2\beta^2(\Delta A_{35}\cos\psi + \Delta A_{34}\sin\psi) - 3\alpha^2(\Delta A_{15}\cos^3\psi - \end{aligned} \tag{B4}$$

$$\Delta A_{34}\sin\psi + (\Delta A_{14} + 2\Delta A_{56})\cos^2\psi\sin\psi + \Delta A_{24}\sin^3\psi +$$
$$(-\Delta A_{35} + (\Delta A_{25} + 2\Delta A_{46})\sin^2\psi)\cos\psi)],$$

$$v_{11} = \frac{2\beta^2}{\alpha^2(\alpha^2-\beta^2)}[\Delta A_{15}\cos^3\psi - \Delta A_{34}\sin\psi + (\Delta A_{14} + 2\Delta A_{56})\cos^2\psi\sin\psi +$$
$$\Delta A_{24}\sin^3\psi + (-\Delta A_{35} + (\Delta A_{25} + 2\Delta A_{46})\sin^2\psi)\cos\psi],$$

and

$$h_1 = \frac{1}{4(\alpha^2-\beta^2)}[-2(\Delta A_{36} + 2\Delta A_{45})\cos 2\psi + (\Delta A_{13} - \Delta A_{23} - \quad \text{(B5)}$$
$$2\Delta A_{44} + 2\Delta A_{55})\sin 2\psi],$$

$$h_2 = \frac{1}{8(\alpha^2-\beta^2)}[-2(\Delta A_{16} - \Delta A_{26})\cos 4\psi + (\Delta A_{11} - 2\Delta A_{13} - \Delta A_{22} + 2\Delta A_{23} +$$
$$4\Delta A_{44} - 4\Delta A_{55})\sin 2\psi + (-2(\Delta A_{16} + \Delta A_{26} - 2\Delta A_{36} - 4\Delta A_{45}) + (\Delta A_{11} -$$
$$2\Delta A_{12} + \Delta A_{22} - 4\Delta A_{66})\sin 2\psi)\cos 2\psi],$$

$$h_3 = \frac{1}{2(\alpha^2-\beta^2)}[\Delta A_{34}\cos\psi - \Delta A_{35}\sin\psi],$$

$$h_4 = \frac{1}{8(\alpha^2-\beta^2)}[(\Delta A_{14} + 3\Delta A_{24} - 4\Delta A_{34} + 2\Delta A_{56})\cos\psi + 3(\Delta A_{14} - \Delta A_{24} +$$
$$2\Delta A_{56})\cos 3\psi + 2(-3\Delta A_{15} + \Delta A_{25} + 2\Delta A_{35} + 2\Delta A_{46} - (3\Delta A_{15} -$$
$$3\Delta A_{25} - 6\Delta A_{46})\cos 2\psi)\sin\psi],$$

$$h_5 = \frac{\alpha}{2\beta(\beta^2-\alpha^2)}[\Delta A_{34}\cos\psi - \Delta A_{35}\sin\psi],$$

$$h_6 = \frac{1}{2\alpha\beta(\alpha^2-\beta^2)}[-(\alpha^2\Delta A_{14} + 2\beta^2\Delta A_{56})\cos^3\psi + (\alpha^2(\Delta A_{15} - 2\Delta A_{46}) +$$
$$2\beta^2(\Delta A_{15} - \Delta A_{25} - \Delta A_{46}))\cos^2\psi\sin\psi + (-(\alpha^2+\beta^2)\Delta A_{35} + (\alpha^2\Delta A_{25} +$$
$$2\beta^2\Delta A_{46})\sin^2\psi)\sin\psi + ((\alpha^2+\beta^2)\Delta A_{34} + (2\beta^2\Delta A_{14} - \alpha^2\Delta A_{24} - 2\beta^2\Delta A_{24} +$$
$$2\alpha^2\Delta A_{56} + 2\beta^2\Delta A_{56})\sin^2\psi)\cos\psi],$$

$$h_7 = \frac{\beta}{8\alpha(\alpha^2-\beta^2)}[(\Delta A_{14} + 3\Delta A_{24} - 4\Delta A_{34} + 2\Delta A_{56})\cos\psi + 3(\Delta A_{14} - \Delta A_{24} +$$
$$2\Delta A_{56})\cos 3\psi + 2(-3\Delta A_{15} + \Delta A_{25} + 2\Delta A_{35} + 2\Delta A_{46} - (3\Delta A_{15} -$$
$$3\Delta A_{25} - 6\Delta A_{46})\cos 2\psi)\sin\psi],$$

$$h_8 = \frac{1}{4\alpha\beta(\alpha^2-\beta^2)}[2(\beta^2\Delta A_{36} + 2\alpha^2\Delta A_{45})\cos 2\psi + (\beta^2(-\Delta A_{13} + \Delta A_{23}) +$$
$$2\alpha^2(\Delta A_{44} - \Delta A_{55}))\sin 2\psi],$$

$$h_9 = \frac{\beta}{8\alpha(\alpha^2-\beta^2)}[2(\Delta A_{16} - \Delta A_{26})\cos(4\psi) + (-\Delta A_{11} + 2\Delta A_{13} + \Delta A_{22} - 2\Delta A_{23} -$$
$$4\Delta A_{44} + 4\Delta A_{55})\sin 2\psi - (-2(\Delta A_{16} + \Delta A_{26} - 2\Delta A_{36} - 4\Delta A_{45}) + (\Delta A_{11} -$$
$$2\Delta A_{12} + \Delta A_{22} - 4\Delta A_{66})\sin 2\psi)\cos 2\psi].$$

Here, i and j denote the incidence and reflection phase angles (respectively), and ψ denotes the azimuthal angle. The quantities $\Delta A_{ij} = A_{ij}^{(2)} - A_{ij}^{(1)}$ are the contrasts of the elastic parameters A_{ij} across the interface, and α, β and ρ^0 are the background parameters.

APPENDIX C: Approximations R_{PS_1} and R_{PS_2} for orthorhombic media

In the text, the R_{PS_1} and R_{PS_2} approximations (38) are derived for orthorhombic media. They contain R_{PSV} and R_{PSH} components (39) which consist of linear combinations of the V_j (j=1,..,5) and H_k (k=1,..,4) terms, respectively. The V_j terms read:

$$V_1 = -\frac{\bar\beta}{\bar\alpha}\frac{\Delta\rho}{\bar\rho} - 2\frac{\bar\beta}{\bar\alpha}\frac{\Delta\beta}{\bar\beta} - \frac{\bar\alpha\bar\beta}{2(\bar\alpha^2-\bar\beta^2)}\Big[\delta_2^{(2)}\cos^2(\psi-\kappa) + \delta_2^{(1)}\sin^2(\psi-\kappa) - \quad \text{(C1)}$$

$$\delta_1^{(2)}\cos^2\psi - \delta_1^{(1)}\sin^2\psi\Big] - 2\frac{\bar\beta}{\bar\alpha}\left[\gamma_2^{(S)}\sin^2(\psi-\kappa) - \gamma_1^{(S)}\sin^2\psi\right],$$

$$V_2 = -\frac{1}{2}\frac{\Delta\rho}{\bar\rho} + \frac{\bar\alpha^2}{2(\bar\alpha^2-\bar\beta^2)}\Big[\delta_2^{(2)}\cos^2(\psi-\kappa) + \delta_2^{(1)}\sin^2(\psi-\kappa) -$$
$$\delta_1^{(2)}\cos^2\psi - \delta_1^{(1)}\sin^2\psi\Big],$$

$$V_3 = -\frac{\bar\alpha\bar\beta}{\bar\alpha^2-\bar\beta^2}\Big[\epsilon_2^{(2)}(\cos^4(\psi-\kappa) + 2\cos^2(\psi-\kappa)\sin^2(\psi-\kappa)) + \epsilon_2^{(1)}\sin^4(\psi-\kappa) -$$
$$\epsilon_1^{(2)}(\cos^4\psi + 2\cos^2\psi\sin^2\psi) - \epsilon_1^{(1)}\sin^4\psi - \delta_2^{(1)}\sin^2(\psi-\kappa) - \delta_2^{(2)}\cos^2(\psi-\kappa)$$
$$+\delta_2^{(3)}\cos^2(\psi-\kappa)\sin^2(\psi-\kappa) + \delta_1^{(1)}\sin^2\psi + \delta_1^{(2)}\cos^2\psi - \delta_1^{(3)}\cos^2\psi\sin^2\psi\Big],$$

$$V_4 = \frac{\bar\beta^2}{\bar\alpha^2}\frac{\Delta\rho}{\bar\rho} + 2\frac{\bar\beta^2}{\bar\alpha^2}\frac{\Delta\beta}{\bar\beta} + \frac{\bar\beta^2}{2(\bar\alpha^2-\bar\beta^2)}\Big[-\delta_2^{(2)}\cos^2(\psi-\kappa) - \delta_2^{(1)}\sin^2(\psi-\kappa) +$$
$$\delta_1^{(2)}\cos^2\psi + \delta_1^{(1)}\sin^2\psi\Big] + \frac{\bar\alpha^2}{\bar\alpha^2-\bar\beta^2}\Big[\epsilon_2^{(2)}(\cos^4(\psi-\kappa) + 2\cos^2(\psi-\kappa)\sin^2(\psi-\kappa))$$
$$+\epsilon_2^{(1)}\sin^4(\psi-\kappa) - \epsilon_1^{(2)}(\cos^4\psi + 2\cos^2\psi\sin^2\psi) - \epsilon_1^{(1)}\sin^4\psi - \delta_2^{(1)}\sin^2(\psi-\kappa) -$$
$$\delta_2^{(2)}\cos^2(\psi-\kappa) + \delta_2^{(3)}\cos^2(\psi-\kappa)\sin^2(\psi-\kappa) + \delta_1^{(1)}\sin^2\psi + \delta_1^{(2)}\cos^2\psi -$$
$$\delta_1^{(3)}\cos^2\psi\sin^2\psi\Big] + 2\frac{\bar\beta^2}{\bar\alpha^2}\left[\gamma_2^{(S)}\sin^2(\psi-\kappa) - \gamma_1^{(S)}\sin^2\psi\right],$$

$$V_5 = -\frac{\bar\beta^2}{\bar\alpha^2-\bar\beta^2}\Big[\epsilon_2^{(2)}(\cos^4(\psi-\kappa) + 2\cos^2(\psi-\kappa)\sin^2(\psi-\kappa))$$
$$+\epsilon_2^{(1)}\sin^4(\psi-\kappa) - \epsilon_1^{(2)}(\cos^4\psi + 2\cos^2\psi\sin^2\psi) - \epsilon_1^{(1)}\sin^4\psi - \delta_2^{(1)}\sin^2(\psi-\kappa) -$$
$$\delta_2^{(2)}\cos^2(\psi-\kappa) + \delta_2^{(3)}\cos^2(\psi-\kappa)\sin^2(\psi-\kappa) + \delta_1^{(1)}\sin^2\psi + \delta_1^{(2)}\cos^2\psi -$$
$$\delta_1^{(3)}\cos^2\psi\sin^2\psi\Big].$$

The H_k terms are as follows:

$$H_1 = \frac{\bar\alpha^2}{4(\bar\alpha^2-\bar\beta^2)}\Big[(\delta_2^{(2)} - \delta_2^{(1)})\sin 2(\psi-\kappa) + (\delta_1^{(1)} - \delta_1^{(2)})\sin 2\psi\Big], \tag{C2}$$

$$H_2 = \frac{\bar\alpha\bar\beta}{4(\bar\alpha^2-\bar\beta^2)}\Big[(\delta_2^{(1)} - \delta_2^{(2)})\sin 2(\psi-\kappa) + (\delta_1^{(2)} - \delta_1^{(1)})\sin 2\psi\Big] +$$
$$\frac{\bar\beta}{\bar\alpha}\left[\gamma_2^{(S)}\sin 2(\psi-\kappa) - \gamma_1^{(S)}\sin 2\psi\right],$$

$$H_3 = \frac{\bar\alpha^2}{2(\bar\alpha^2-\bar\beta^2)}\Big[\Big[\Big[\delta_2^{(1)} - \delta_2^{(2)} - \delta_2^{(3)}(\cos^2(\psi-\kappa) - \sin^2(\psi-\kappa)) +$$
$$2(\epsilon_2^{(2)} - \epsilon_2^{(1)})\sin^2(\psi-\kappa)\Big]\sin(\psi-\kappa)\cos(\psi-\kappa) + \Big[-\delta_1^{(1)} + \delta_1^{(2)} +$$
$$\delta_1^{(3)}(\cos^2\psi - \sin^2\psi) - 2(\epsilon_1^{(2)} - \epsilon_1^{(1)})\sin^2\psi\Big]\sin\psi\cos\psi\Big],$$

$$H_4 = -\frac{\bar\alpha\bar\beta}{2(\bar\alpha^2-\bar\beta^2)}\Big[\Big[\Big[\delta_2^{(1)} - \delta_2^{(2)} - \delta_2^{(3)}(\cos^2(\psi-\kappa) - \sin^2(\psi-\kappa)) +$$
$$2(\epsilon_2^{(2)} - \epsilon_2^{(1)})\sin^2(\psi-\kappa)\Big]\sin(\psi-\kappa)\cos(\psi-\kappa) + \Big[-\delta_1^{(1)} + \delta_1^{(2)} +$$
$$\delta_1^{(3)}(\cos^2\psi - \sin^2\psi) - 2(\epsilon_1^{(2)} - \epsilon_1^{(1)})\sin^2\psi\Big]\sin\psi\cos\psi\Big].$$

Here, $\Delta x = x^{(2)} - x^{(1)}$ denotes the contrast of the parameter x across the interface. See the text for definitions of the other quantities. The reference coordinate system is associated with the symmetry planes of the incidence orthorhombic medium.

APPENDIX D: Polarization angle Φ

Here, I evaluate theoretical expressions for $\cos\Phi$ and $\sin\Phi$ required in formulas for R_{PS_1}, R_{PS_2} coefficients.

Jech and Pšenčík (1989), and Pšenčík (1998) derived general expressions that can be specified for a particular anisotropic symmetry. Adopting the convention introduced in Figure 1b yields for an orthorhombic incidence medium:

$$\begin{aligned} \cos\Phi &= \left[\frac{1}{2}(1+\frac{A}{D})\right]^{1/2}, \\ \sin\Phi &= \frac{B}{|B|}\left[\frac{1}{2}(1-\frac{A}{D})\right]^{1/2}, \end{aligned} \tag{D1}$$

for $B \neq 0$, or

$$\cos\Phi = 1, \qquad \sin\Phi = 0 \qquad (B=0). \tag{D2}$$

In (D1),

$$D \equiv [A^2 + 4B^2]^{1/2} \tag{D3}$$

and

$$\begin{aligned} A \equiv\ & 2A_{33}^{(1)}(\epsilon_1^{(2)}\cos^2\psi - \tilde{\delta}_1^{(2)})\cos^2\psi\cos^2 j\sin^2 j + \\ & 2A_{33}^{(1)}(\epsilon_1^{(1)}\sin^2\psi - \tilde{\delta}_1^{(1)})\sin^2\psi\cos^2 j\sin^2 j + \\ & 2A_{33}^{(1)}(1+2\epsilon_1^{(2)})\tilde{\delta}_1^{(3)}\cos^2\psi\sin^2\psi(\cos^2 j+1)\sin^2 j + \\ & 4A_{33}^{(1)}\epsilon_1^{(2)}\cos^2\psi\sin^2\psi\cos^2 j\sin^2 j + \\ & 2A_{33}^{(1)}(\epsilon_1^{(2)}-\epsilon_1^{(1)})\cos^2\psi\sin^2\psi\sin^2 j - \\ & 2A_{55}^{(1)}\gamma_1^{(1)}\sin^2\psi\sin^2 j - \\ & 2A_{55}^{(1)}\gamma_1^{(S)}\cos^2(2\psi) - \\ & 2A_{55}^{(1)}(\gamma_1^{(1)}-\gamma_1^{(S)})\cos^2\psi\sin^2 j, \end{aligned} \tag{D4}$$

$$\begin{aligned} B \equiv\ & A_{33}^{(1)}(1+2\epsilon_1^{(2)})\tilde{\delta}_1^{(3)}\cos\psi\sin\psi\cos 2\psi\cos j\sin^2 j + \\ & 2A_{33}^{(1)}(\epsilon_1^{(1)}-\epsilon_1^{(2)})\cos\psi\sin^3\psi\cos j\sin^2 j + \\ & A_{33}^{(1)}(\tilde{\delta}_1^{(2)}-\tilde{\delta}_1^{(1)})\cos\psi\sin\psi\cos j\sin^2 j + \\ & 2A_{55}^{(1)}\gamma_1^{(S)}\cos\psi\sin\psi\cos j, \end{aligned} \tag{D5}$$

where $\gamma_1^{(1)} \equiv (A_{66}^{(1)} - A_{55}^{(1)})/2A_{55}^{(1)}$ (Tsvankin, 1997b), and all the other quantities are defined in the text.

It can be shown that $\cos\Phi$ and $\sin\Phi$ are singular ($D=0$) for the directions of the reflected-wave slowness vector corresponding to S-wave singularities, where the S_1- and S_2-wave velocities are identical. For such cases, neither equations (D1) nor the R_{PS_1} and R_{PS_2} approximations (38) can be used.

We can proceed in exactly the same way as above, if the incidence halfspace is HTI. However, we can also use the fact, that the polarizations of S-waves propagating in HTI media are known. One of the waves is always polarized within the plane formed by the slowness vector and the horizontal symmetry axis, while the other is polarized in the isotropy (vertical) plane. These geometrical relationships make it possible to derive purely "geometrical" expressions for $\cos\Phi$ and $\sin\Phi$ that do not contain any medium parameters:

$$\begin{aligned} \cos\Phi &= \frac{\cos j\cos\psi}{\sqrt{1-\sin^2 j\cos^2\psi}}, \\ \sin\Phi &= \frac{-\sin\psi}{\sqrt{1-\sin^2 j\cos^2\psi}}. \end{aligned} \tag{D6}$$

As before, j and ψ denote the S-wave reflection phase angle and the azimuth of the incidence plane, respectively. Equations (D6) are more stable than (D1), with the only singular point for $j = 90^\circ$ and $\psi = 0^\circ$. Obviously, the incidence angle $j = 90^\circ$ is far beyond the area of applicability of the approximations.

In the case of a VTI incidence halfspace, the situation is considerably simpler. One S-wave is polarized in the incidence plane (SV) and the other is perpendicular (SH). Thus it immediately follows

$$\cos\Phi = 1, \qquad \sin\Phi = 0. \tag{D7}$$

From equations (D7), R_{PS_1} for VTI media represents the reflection coefficient of the P-SV wave (polarized in the incidence plane) and R_{PS_2} represents the reflection coefficient of the P-SH wave (polarized horizontally). Notice that such a P-SH conversion is generated if the reflecting halfspace has HTI or orthorhombic symmetry [equations (C1) and (C2)].

Equations (D7) also hold for a purely isotropic incidence medium. In that case, R_{PS_1} and R_{PS_2} correspond to the SV and SH components of the S-wave, respectively; both components travel with the same velocity.